

Master thesis in quality in analytical laboratories

**Process Monitoring of Continuous Flow Organic Syntheses  
by means of Inline Fiber Optical Raman Spectroscopy**



**Muhammad Saif Ur Rehman  
Kjemisk institutt  
Universitetet i Bergen  
2010**

To  
**Ameena Saeed Khattak**

## **Acknowledgements**

All the praises and thanks are for Almighty ALLAH Who bestowed me with the potential and ability to contribute a little to the existing scientific knowledge.

I feel that I do not own this dissertation solely. Honestly, it is the effort of all those people who take care of me. I want to pay my special complements to Prof. Bjorn Grung and Prof. Hans-Rene Bjorsvik for their continuous guidance and encouragement throughout this project. Dr. Egil Nodland and Dagfinn Sleveland, are thanked for their valuable support inside and outside the laboratory.

I will especially express my gratitude to Aamir Ali for his company and encouragement during my stay in Bergen. I acknowledge my Pakistani fellows at Fantoft especially Mr. Sajjad Zaki and his family, who took care of me.

I have to thank the European Union for providing me an EMQAL studentship and an opportunity to stay and learn in Europe. The university and city of Bergen is acknowledged for its weather and people.

## **Abstract**

The objective of the current study was to investigate the feasibility of the inline optical fiber Raman spectroscopy as a tool for the process monitoring of the continuous flow organic syntheses. The synthesis of 2-bromo-3,4,5-trimethoxytoluene (product) was studied as a model reaction under a set of different conditions. The reaction was carried out under the batch as well as in the multi jet oscillating disc (MJOD) milli reactor. The reaction was varied by doubling the concentration of the substrate; 3,4,5-trimethoxytoluene (0.15M, 0.3M and 0.6M) whereas the concentration of the solvent (acetic anhydride) was kept constant. The Raman instrument was adjusted to record five spectra per minute. The recorded spectral data was then preprocessed employing the second order differentiation to minimize the band overlapping in the spectra. Multivariate data analysis namely, Principal Component Analysis (PCA), was used to evaluate the spectra due to the presence of overlapping bands for the purpose of process monitoring. The measurement system was tested against the possible process disturbances, the oscillator and the feeding pumps. PCA showed that these disturbances had no impact on the measurement system. The Raman instrument successfully monitored the different organic reactions and discriminated them on the basis of the type of variation occurred. The Raman frequencies; 675, 1050 and 550  $\text{cm}^{-1}$  were assigned to the solvent, substrate and the product. The various reactions undergoing any disagreement were differentiated from the normal reactions mainly due to the temperature effect, malfunctioning of the pump, lower conversion of the substrate, lower yield of the product, formation of the intermediates etc. The offline results obtained from the NMR spectroscopy verified the outcomes of Raman measurements. Thus, it was concluded that the optical fiber Raman spectroscopy proved to be a reliable, rapid and sensitive inline analytical method for the monitoring of the organic processes. Raman spectroscopy along with an appropriate chemometric tool could be employed as a Process Analytical Technology (PAT) in the pharmaceutical and fine chemical industry.

## Table of Contents

<b>Acknowledgement.....</b>	<b>III</b>	
<b>Abstract.....</b>	<b>IV</b>	
<b>Table of Contents.....</b>	<b>V</b>	
<b>List of Abbreviations.....</b>	<b>VII</b>	
<b>1.</b>	<b>Introduction.....</b>	<b>1</b>
<b>2.</b>	<b>Theory.....</b>	<b>3</b>
2.1	Optical Fiber Spectroscopy.....	3
2.2	Raman Spectroscopy.....	4
2.3	Model Development.....	6
2.4	Pretreatment of spectral data.....	6
2.5	Multivariate analysis methods.....	8
2.6	Principal component analysis.....	9
2.7	Process control.....	9
<b>3.</b>	<b>Materials and Methods.....</b>	<b>12</b>
3.1	Chemicals.....	12
3.2	Synthesis of 2-bromo-3,4,5-trimethoxytoluene.....	12
3.3	Experimental.....	13
3.3.1	Batch reaction.....	13
3.3.2	Multi jet oscillating disc milli reactor.....	13
3.4	Raman spectroscopy .....	15
3.5	Data acquisition and analysis.....	15
<b>4.</b>	<b>Result and Discussion.....</b>	<b>17</b>
4.1	Disturbance diagnosis for MJOD reactor.....	17
4.1.1	Oscillator effect.....	17
4.1.2	Pump effect.....	17
4.2	Raman spectra.....	19
4.3	Monitoring the synthesis of 2-bromo-3,4,5-trimethoxytoluene...	20
4.3.1	Reaction 1.....	20
4.3.1.1	Batch reaction.....	20
4.3.1.2	MJOD reactor.....	23
4.3.2	Reaction 2.....	25
4.3.2.1	Batch reaction.....	25
4.3.2.2	MJOD reactor.....	29
4.3.3	Reaction 3.....	31
4.3.3.1	Batch reaction... ..	31
4.3.3.2	Reactor reaction.....	34

<b>5.</b>	<b>Conclusions and Future Perspectives.....</b>	<b>40</b>
<b>6.</b>	<b>References.....</b>	<b>41</b>
<b>7.</b>	<b>Appendix 1.....</b>	<b>44</b>

## **List of Abbreviations**

MJOD	Multi Jet Oscillation Disc
PCA	Principal Component Analysis
PAT	Process Analytical Technology
FDA	US Food and Drug Administration
LC	Liquid Chromatography
GC	Gas Chromatography
NIR	Near Infrared
FT	Fourier Transformed
QbD	Quality by Design
MSC	Multiple Scatter Correction
SNV	Standard Normal Vitiate
DT	De-trending
SG	Savitzky–Golay
MLR	Multilinear Regression
PCR	Principal Component Regression
PLS	Partial Least Square
PCs	Principal Components
MSPC	Multivariate Statistical Process Control
CUSUM	Cumulative Sum
EWMA	Multivariate Exponentially Weighted Moving Average
SMART	Simultaneous Scores Monitoring and Residual Tracking
NMR	Nuclear Magnetic Resonance
RTR	Real Time Release

## 1. Introduction

Traditionally organic syntheses and organic processes have been conducted by using batch protocols due to their flexibility and versatility for cost-effective manufacture of small quantities of chemicals with short product lifetime. Batch reactions are carried out in the laboratory, by means of small glass flasks (mL–L), while on the industrial scale in glass-lined stirred tank reactors (some few gallons up to several m<sup>3</sup>). The batch production of pharmaceutical chemicals involves several intermediate reactions. This inherent character of the pharmaceutical syntheses leads to time-consuming and costly production processes. Moreover, offline analytical techniques like chromatography and spectroscopy are employed for the reaction monitoring and quality control of such processes which prove another bottleneck for timely production of quality product. Therefore, Process Analytical Technology (PAT) initiative of the US Food and Drug Administration (FDA) cannot be implemented in the traditional batch production processes<sup>1</sup>.

The pharmaceutical and fine chemical industry is continuously emphasizing on the research and development of more efficient and economical in order to maintain their competitive edge in the growing global health care market<sup>2</sup>. A continuous production process shares several intrinsic advantages over the batch processes which include higher productivity, improved safety, reduced manufacturing costs, and reduction or elimination of inventories than batch production. Furthermore, continuous production can produce a pre specified quality product employing an appropriate process control strategy against the process disturbances like variations in the quality of the raw materials, process variables etc<sup>1</sup>. These advantages along with the recent developments in the micro-reactor technology have motivated the pharmaceutical industry to investigate continuous processing as an innovative alternative.

During the recent years flow chemistry has been adopted for the use in organic synthesis and organic processes. Thus, continuous flow reactors have turned to be an important approach for performing organic synthesis, being both in the academic laboratory as well as in the organic process environment for the production of various fine and pharmaceutical chemicals. Micro-reactor technology has induced a revolution in the pharmaceutical industry as it can get benefits of continuous processing with some flexibility<sup>3</sup>. Additionally, it can result in the potential savings associated with the R&D costs and time. Micro-reactors typically posses the dimensions in the sub-millimeter range and hold-up volumes in the micro liters. Improved heat and mass transfer and appropriate process control can be obtained using high surface area to volume ratio<sup>2</sup>. However, the wall effect becomes more pronounced when high surface area to volume ratio is employed in the micro-reactors. Moreover, chemicals adsorbed on the channel walls result in the loss of the product and decreased capacity of the reactor. The smaller production capacity proves another challenge to the microreactor technology<sup>4</sup>.

Multi-Jet Oscillating Disc (MJOD) milli-reactor is an innovative alternative technology to the micro reactor technology. It addresses all of the problems associated with the micro reactors. It is

novel applied technology which accelerates the flow organic synthesis in the continuous macro (35-50 mL) experimental scale (on milli-scale rather than micro-scale). The MJOD milli-reactor system ensures higher throughput due to the scale difference as compared to the micro-reactor systems. However, it still sustains the major advantages associated with the micro-reactor technology. The mjud milli-reactor system is very flexible and can handle heterogeneous reactions without the clogging of small perforated discs inside the reactor. Thus, it can be employed for several types of reactions<sup>5</sup>. Even though many advantages of such reactor system have been noticed, still it requires a rapid and reliable analytical system which can ensure a better process understanding and hence, a better process control and the quality of the product. PAT integrated with the MJOD milli-reactor technology can provide a better process understanding which can be used for the process development, optimization, scale-up, technology transfer and efficient process control. Moreover, it will ensure continuous real time information about the predefined product quality<sup>6</sup>.

This project will investigate the feasibility of the fiber optical Raman spectroscopy coupled with multivariate mathematical and statistical methods for the purpose of the monitoring a set of selected organic syntheses. The organic reactions will be carried out under the batch conditions to develop the reaction profiles as well as in the MJOD mill reactor to monitor the process. The recorded data will then be subjected to the subsequent multivariate analysis; Principal Component Analysis (PCA) to identify any patterns among the spectra. The potential process disturbances; oscillator and pump system, will be studied to note their effect on the measurement system. Subsequent with the spectroscopic monitoring, samples will also be withdrawn for off-line analyses using NMR spectroscopy.

## **2. Theory**

Continuous micro-reaction technology has proved to be a promising technology due to its salient features. It involves intensification of chemical processes and continuous than the conventional batch system. This technology if applied to produce fine chemicals can increase the production manifolds than the batch processes. Besides a higher chemical throughput, a reliable and rapid analytical system is mandatory to ensure the quality of the produced chemicals for their intended use. This integrated approach can force a revolution in the fine chemical industry. The inline analytical techniques can be one option for such challenge. These techniques are directly employed on the process streams i.e. reactor, feed line or product line etc. using fiber optical probes. Hence, these techniques can endorse an even faster monitoring of the process<sup>7</sup> than the time consuming offline techniques. Reaction monitoring is an important area for chemical process development. The synthesis of pharmaceuticals is comprised of many intermediate reaction steps which are carried out in a series<sup>8</sup>. Inline analytical techniques, on the one hand, provide much faster qualitative information than usual about the state of the continuous process and on the other hand, they can identify and locate existing process fluctuations that may help to control the process and ultimately ensure the quality of the product<sup>7-10</sup>.

The interest in developing rapid, reliable and relevant analytical methods for fine chemicals has been increased to ensure their pre specified quality. Offline analysis like liquid chromatography (LC) or gas chromatography (GC) is a real bottleneck during the continuous production. Inline analysis can overcome many inherent problems of these offline techniques. Process optimization, product quality and process control measures can easily be ensured using these techniques with multivariate data analysis<sup>11</sup>.

The pharmaceutical industry has shown keen interest in the development and adaptation of inline spectroscopic techniques for process monitoring following the FDA guidelines on PAT<sup>12</sup>. PAT can improve the productivity through better process understanding. Thus, PAT can enhance the quality of pharmaceutical products with reduced production cost and will ensure a new product release approach; real-time release (RTR), than conventional quality assurance methods. RTR ensures the intended quality of the product by removing traditional end-product testing step. Ultimately, PAT can play a leading role in the improvement of the health care management around the globe<sup>13</sup>.

### **2.1 Optical fiber spectroscopy**

Spectroscopy is an important tool for the monitoring of various chemical processes due to its fast response time and ability to perform multi-component measurements. It permits the detection of side products if produced during the reaction. Spectroscopic techniques coupled with fiber optics make an ideal combination for the real time remote monitoring of chemical processes. The fiber optical system isolates the instrument from the processing setup and minimizes any kind of risks associated with vibrational and electrical disturbance. These advantages make the optical fiber

spectroscopy an ultimate choice for process monitoring than the offline analytical techniques. Vibrational spectroscopic techniques either near-infrared (NIR) or Raman spectroscopy are mostly used for this purpose. Perhaps, inline fiber optical spectroscopy will be developed as the standard equipment for the process industry in future<sup>8-9</sup>.

## 2.2 Raman spectroscopy

The modern Raman instrument carries many salient features which make them an ultimate choice for the process monitoring. These features include fiber optical probes, compact design, efficient detectors, and computers with fast data acquisition and analysis software. The laser induced Raman spectroscopy is a powerful tool preferred for *in-situ* monitoring of the organic reactions<sup>14-16</sup>.

When a monochromatic light falls on a substance, some radiations are absorbed by the substance while remaining radiations get scattered with the same frequency of the incident light. This kind of scattering is known as Rayleigh scattering. A small fraction of the incident photons experience some shift in their frequency. These photons lose their energy when they interact with the centre of the molecule. This interaction is called Stokes scattering. There is another group of photons which contain more energy than the exciting radiation and are known as anti-Stokes photons (Fig. 2.1). The increase or decrease in the energy of the scattered photons depends on the molecular vibrations in its ground state. Only Stokes scattering is measured in the Raman spectroscopy<sup>17</sup>. A standard Raman spectrum ranges between 0-3500cm<sup>-1</sup> wave numbers (Fig. 2)<sup>18</sup>. The molecular motion and types of atoms present in the chemical bond are responsible for the position and intensity of a vibration in the spectrum<sup>19</sup>.

Two main techniques are used to collect the Raman spectra: dispersive and Fourier transformed Raman (FT-Raman). The two techniques differ in the use of laser and, the detection and analysis of Raman scattering. The selection of the technique entirely depends on the nature of the sample<sup>20</sup>. Raman-spectroscopy was reported as the most robust method for the one-phase reaction system. The precision was found to be the highest within the calibration space<sup>7</sup>. Lee *et al*<sup>21</sup>, successfully monitored the imine formation employing the Raman spectroscopy. It was found that the measurement system was not only capable of reaction monitoring but it also provided information related to the substitution effect of aromatic ring. Intermolecular interactions and the reactivities of the reactants were understood on the basis of recorded Raman spectra.

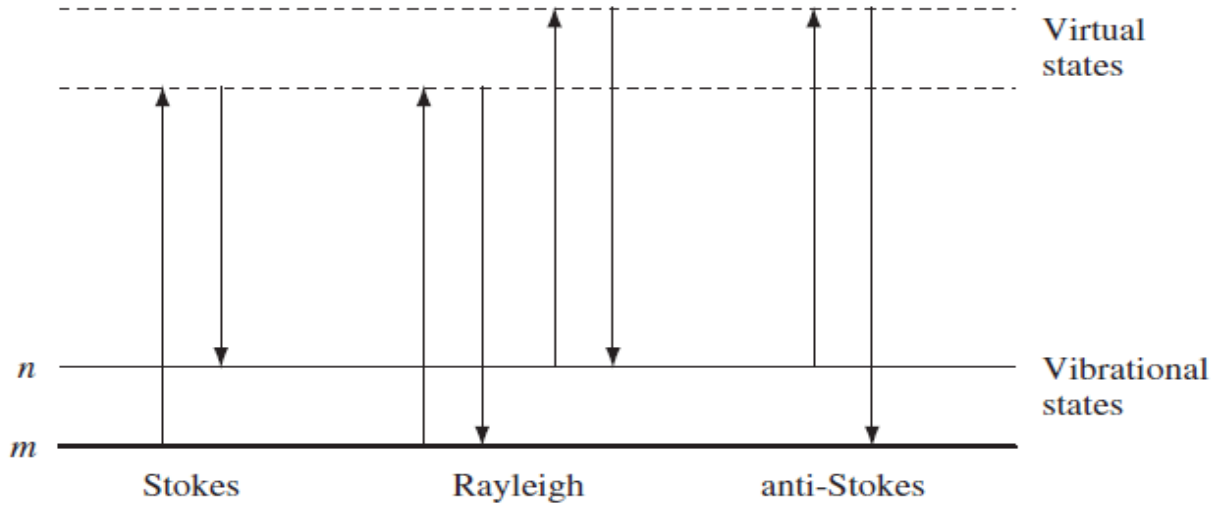


**Figure 2.1:** Various scattering processes (Rayleigh and Raman scattering). The lowest energy vibrational state *m* is shown at the foot with states of increasing energy above it. Both the low energy (upward arrows) and the scattered energy (downward arrows) have much larger energies than the energy of a vibration<sup>17</sup>.

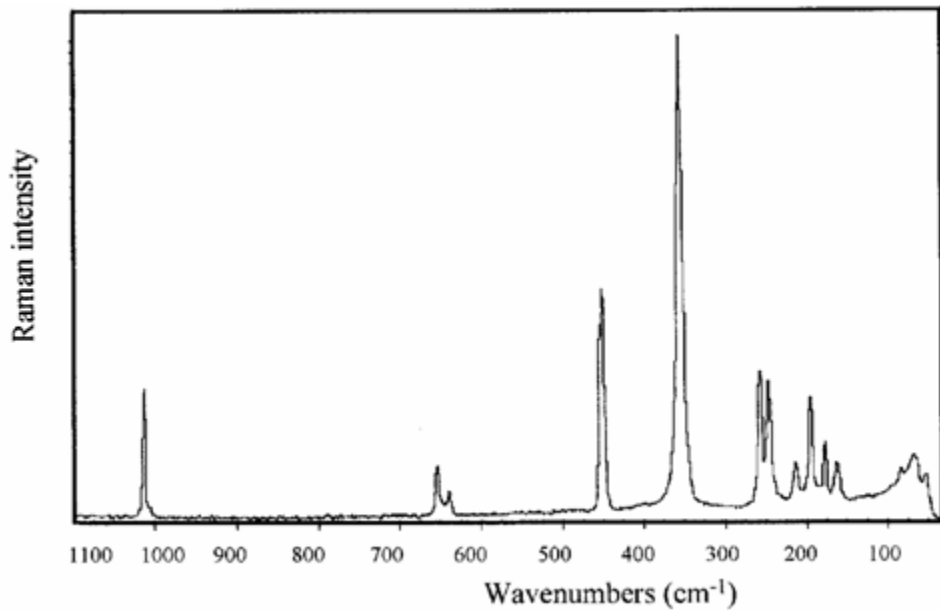


**Figure 2.2:** The Raman spectrum<sup>18</sup> of  $\text{PCl}_4\text{VOCl}_4$

Calibration models are often used to correlate spectral measurement with the desired properties in process monitoring however, the process variability (temperature, pressure, heterogeneity etc.) poses a major challenge. According to Reis *et al*<sup>9</sup>, emulsion polymerization is a heterogeneous process that undergoes significant changes over the period of time. Thus, the model must account for the same behavior that is shown by the Raman spectra during the polymerization process. These spectra can be obtained either from the samples taken during the reaction or by using synthetic samples. The first option usually produces good results for representative process monitoring. Normalization should be applied during quantitative analysis to compensate for process variability due to the fluctuations. It increases stability of the calibration model<sup>19</sup>.

### **2.3 Model development**

Data analysis has become more crucial in the pharmaceutical industry due to the adaptation of PAT in the recent years. Industrial processes and their products exhibit multivariate character. Thus, multivariate models are applied to monitor the process and product quality. Multivariate analysis is responsible for model creation, validation, and its implementation. Such model can be applied successfully if it is robust and the input data is consistent with the data that has been used for the model development.

Quality-by-Design (QbD) approach is used to add quality control elements into a new product or process. For a QbD model, it is usually applied to small scale process in order to check behavior of the process under selected variables. Typically, the development phase involves experimentation and statistical analysis which correlate process variables with some quality parameters of interest. The model can predict a given quality attribute of the process/product. This approach also identifies the critical control points in the process and results in the development of a robust process with proper control<sup>22</sup>.

### **2.4 Pretreatment of spectral data**

Preprocessing is an important part of the spectroscopic data analysis. Appropriate preprocessing technique reduces the variability of measurements due to the instrumental drift, sample heterogeneity etc<sup>23</sup>. Blanco and Villarroya<sup>24</sup> noticed that the spectra of solid samples were affected by the physical properties of sample. This posed some problems in the evaluation of the properties which were independent of physical attributes (raw materials and determination of composition). In this case, spectral pretreatment minimized irrelevant information in the spectra. Therefore, model accuracy and robustness depends on the application of an appropriate pretreatment technique<sup>25</sup>. Several data preprocessing techniques have been successfully applied to spectroscopic applications which include normalization<sup>26</sup>, baseline/scatter correction<sup>27-28</sup>, differentiation (usually first or second order derivatives)<sup>29</sup>, multiplicative scatter correction (MSC)<sup>30</sup>, standard normal variate (SNV), de-trending (DT)<sup>31</sup> or their combination.

Differentiation is used to increase the resolution and minimize the background absorption in the spectroscopic techniques when many overlapping peaks are observed. The first derivative assists in locating the position of a broad peak and eliminates the effect of additive constant background. The second derivative pinpoints two different peaks and their positions as well. It removes any effect related to the baseline slope variation as well as any additive effects. Differentiation requires intense computation and tends to increase the noise. Therefore low signal to noise ratio is usually preferred. These problems can be handled using the Savitzky–Golay (SG) coefficients. The SG algorithm is widely used for differentiation. The spectral data is fitted with polynomial of specified degree to generate a desired degree differential. In order to ensure that the calculated derivative stands for the actual behavior of the spectrum, the width of the moving window should be defined correctly<sup>29,32</sup>. Laasonen *et al*<sup>33</sup>, applied an SG second derivative on the absorbance spectra of caffeine in order to increase the resolution by baseline correction and the removal of overlapping peaks. Mean centering and SNV correction were applied to eliminate any offset and the major effects related with the light scattering. The noisy regions in the data were removed by applying the wave number selection. The effect of preprocessing is explained in Fig. 2.3-2.4<sup>34</sup>.

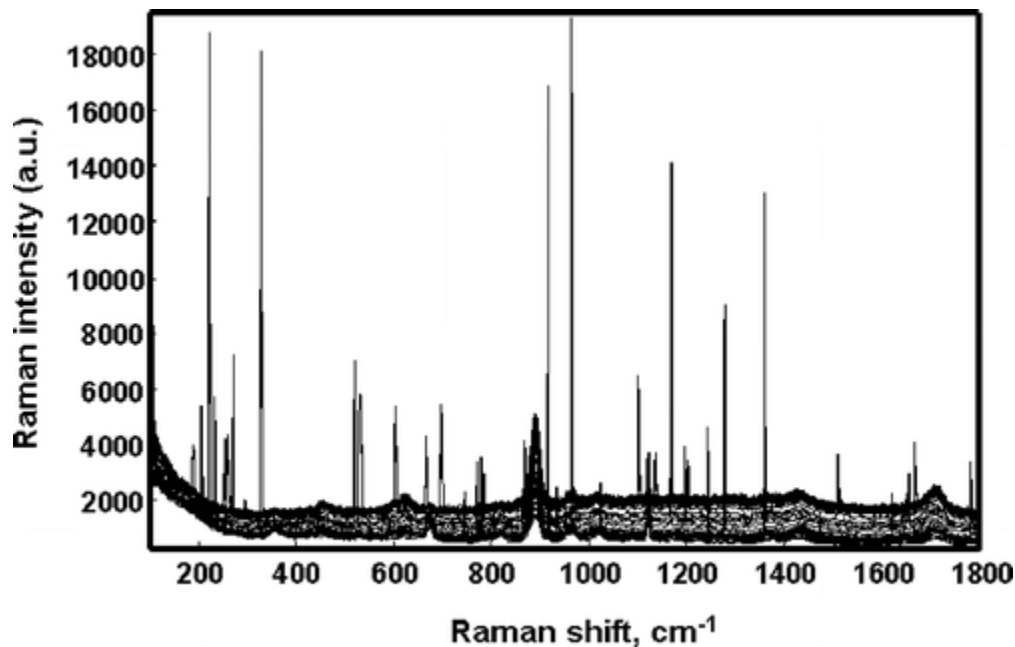


**Figure 2.3:** Raw Raman spectra before any spectral preprocessing<sup>34</sup>

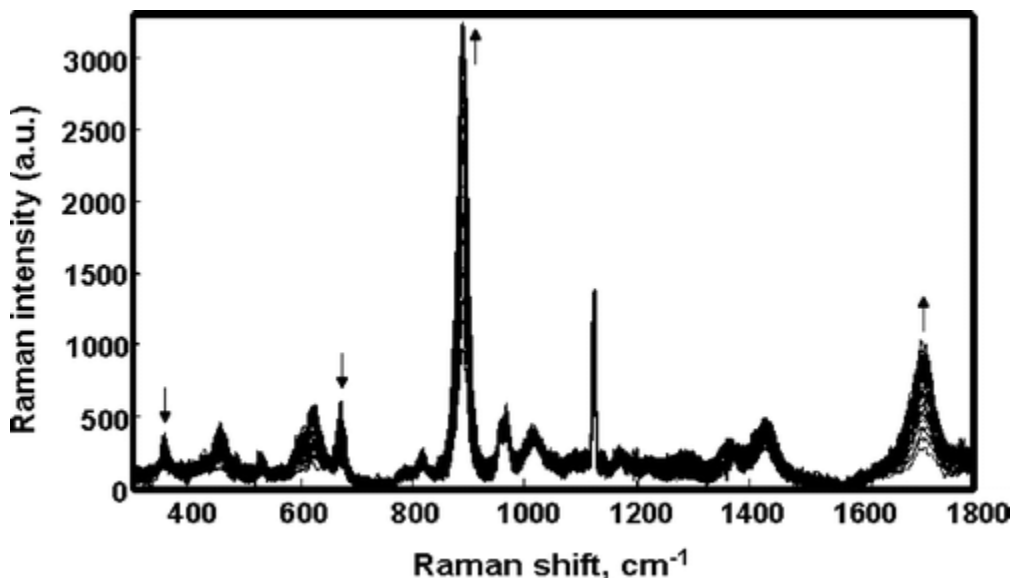


**Figure 2.4:** Raman spectra after spectral preprocessing<sup>34</sup>

## 2.5 Multivariate analysis methods

Multivariate methods are used to build models which can predict the attributes of unknown samples using similar set of conditions. These methods can be classified according to their application. The selection of an appropriate method depends on the requirements, properties of the samples and the system. The models are verified for their prediction using the samples obtained under the same conditions (acquisition and pretreatment) used to build the model<sup>24</sup>.

Raman spectra contain chemical and physical information that can be used for the process monitoring and prediction of product quality. Differences among the samples cannot be identified with the naked eye. However, the modern instruments provide enormous data that can be processed to give valuable chemical information. Chemometric tools are often used to extract such information from the spectral data. Chemometrics and spectroscopy have proven complementary to each other<sup>24,35</sup>. Chemometrics is often used for exploratory data analysis and multivariate statistical process control<sup>36-37</sup>. These techniques are based on finding the latent variable (principal component analysis) as discussed in the literature. Other techniques involving multilinear regression (MLR), principal component regression (PCR), and partial least-squares (PLS)<sup>27-28, 38-40</sup> are also employed for the process and product quality monitoring using prediction models<sup>24</sup>.

## **2.6 Principle component analysis (PCA)**

PCA searches for some pattern among the samples and reduces the dimensions of original data set to a few uncorrelated variables containing only relevant information from the samples<sup>41</sup>. PCA describes relationship among the samples (score values) and among the variables (loadings) and between samples and variables (biplot). PCA searches for directions of maximum variability in the data matrix and extracts the latent variables known as principal components (PCs). These PCs are new variables which explain almost similar information as the original data<sup>24</sup>. PCs are linear combination of the original variables and orthogonal to each other. The first PC explains the maximum variability in the data whereas subsequent PCs explain decreasing levels of variability. Final PCs are ignored owing to the assumption that they represent only noise in the data.

The first principal component is defined as

$$X = t_1 p'_1 + t_2 p'_2 + \dots + t_A p'_A + E$$

where ‘t’ is known as score vector , ‘p’ is the loading vector, ‘A’ denotes number of PCs, E represents residual matrix and X is the original data matrix. The scores are mathematically orthogonal to each other and explain relationship among the samples. The loadings explain relationship among the variables of data. The number of PCs can be found using cross validation approach. A few numbers of PCs are used in process monitoring of organic synthesis than number of spectra and frequencies<sup>42-43</sup>.

PCA and PLS are commonly used in NIR spectroscopy due to the features of spectral data like dimensionality, collinearity and noise<sup>44-45</sup>. However, these multivariate methods are not applicable to Raman data as in the case of NIR because the Raman bands are sharp and selective than the NIR spectra. Therefore, univariate methods are preferred in the case of Raman data analysis. Svensson et al<sup>42</sup>., showed that when Raman spectra with selective peaks were analyzed, PCA and PLS presented similar results like the univariate techniques. However, when complex reaction mixture with several large and similar molecules was studied, a more complex Raman spectra comprising of overlapped bands were obtained. Such complex data was treated with multivariate methods to extract the chemical information. Multivariate methods in the Raman spectroscopy were also used for quantitative calibration purposes<sup>46</sup>.

## **2.7 Process control**

The production of quality product is the desired objective of any manufacturing system. Therefore, inline process monitoring techniques are preferred so as to minimize the risk of off specified production by identifying crucial process disturbances and proposing early warning of process faults. The desired product quality can be achieved by early detection followed by the

location of the disturbance. Most industrial processes and their products demonstrate multivariate character. Thus, the application of univariate analysis can cause erroneous process control<sup>43</sup>.

The multivariate methods build the model that correlates product quality with process attributes. One of the possible ways of representing such analysis is the combined control charts where the scores are plotted along with the residuals. This approach ensures multivariate quality control limits than univariate alarm limits. The multivariate quality control charts will ensure the quality product based on multivariate attributes of the manufacturing process<sup>47</sup>.

PCA and PLS can be used for the development of process control based on continuous process monitoring. The scores describe multivariate characteristics of the samples and contain less noise than the original variables, so they are an ideal option to build the multivariate control charts for the process. Thus, it provides a more efficient way of the process monitoring and defines normal or inconsistent process points over the period of time. Multivariate control charts have been discussed in detail in the literature<sup>44</sup>. These techniques have been successfully implemented for process monitoring, understanding, and troubleshooting. They have provided a basis for multivariate statistical process control (MSPC). MSPC monitors and ensures the quality of the process and the product in real time<sup>48-49</sup>.

MSPC schemes using PCA are based on the assumptions that the process variables are normally distributed and linearly correlated. MSPC is usually performed under steady-state conditions due to the aforementioned assumptions. The nonlinearity of the process, autocorrelation, process dynamics, and changes in operating conditions pose some problems for MSPC. Alternatively, the dynamic, nonlinear, or adaptive MSPC approaches can be applied to avoid any limitation<sup>50</sup>.

Since the PC scores contain multivariate information so they produce information about the status of a running process. They follow normal distribution as long the process is working as desired. Therefore, any change in the normal behavior of the process can be identified by finding normality of the scores using the test statistics Hotelling's  $T^2$ . It provides information about the observation/samples which follow multivariate normality. It is based on the multivariate generalization of Student's  $t$ -test. A graphical representation of the Hotelling's  $T^2$  in a two PCs model is given in Fig. 2.5. The Hotelling  $T^2$  for observation  $i$ , based on  $A$  components is:

$$T_i^2 = \sum_{a=1}^A \frac{t_{ia}^2}{s_{ia}^2}$$

where  $s_{ia}^2$  represents variance of score vector given by PC model.

$T_i^2 \times N(N-A)/A(N^2-1)$  gives F distributed with respect to A and N-A degrees of freedom. Thus if :

$$T_i^2 > A(N^2-1)/N(N-A)/*F_{critical(A, N-A, \alpha)}$$

Then 'i' sample will be out of the 95% tolerance level of the PC model. The tolerance space for a two dimensional score plot (say for  $t_1$  and  $t_2$ ) will be an ellipse given as

$$s_{ta}^2 \times F_{2, N-2, \alpha} \times 2(N^2-1)/(N(N-2))^{1/2}$$

Thus Hotelling  $T^2$  can be used to define a control region for scores in a two dimensional PC model space. This approach can help in the identification of samples which behave different than normal. Resultantly, the process can be continuously monitored for any potential change in the system. Besides this approach, there are several MSPC methods like multivariate Shewhart chart, multivariate Cumulative Sum (CUSUM) chart, multivariate exponentially weighted moving average (EWMA) and simultaneous scores monitoring and residual tracking (SMART) charts<sup>47</sup>.

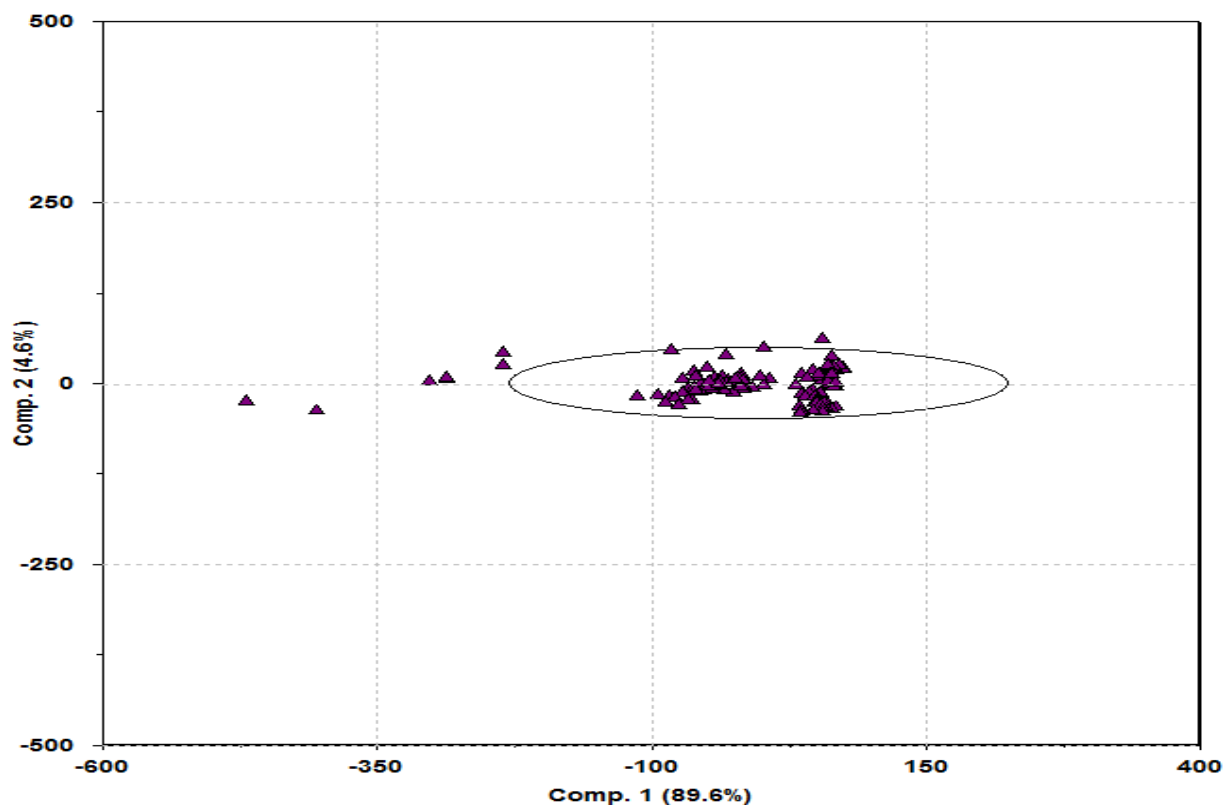


**Figure 2.5:** Two PCs score plot with the Hotelling  $T^2$  ellipse

### 3. Materials and Methods

#### 3.1 Chemicals

The chemicals used in the current study include: 3,4,5-trimethoxytoluene ( $\geq 98\%$ , TCI Zwijndrecht), acetic anhydride ( $\geq 99\%$ , Riede-deHaen, Germany), KBr ( $\geq 99\%$ , Sigma-Aldrich, Germany) and nitric acid (65%, Merck, Germany). All these chemicals were purchased commercially and used without further purification.

#### 3.2 Synthesis of 2-bromo-3,4,5-trimethoxytoluene

The protocol followed for the synthesis of 2-bromo-3,4,5-trimethoxytoluene (2a) was developed in our laboratory and is given in Fig. 1. The detailed procedure can be found in the literature<sup>51</sup>. Briefly, the substrate; 3,4,5-trimethoxytoluene (1a), and KBr were mixed with acetic anhydride. Nitric acid was added drop wise in acetic anhydride to achieve better Br<sub>2</sub> production and selectivity. The oxidant was added at 20 °C, and the temperature was kept constant throughout the bromination reaction. The reaction mixture was stirred for 45 minutes at 20°C.

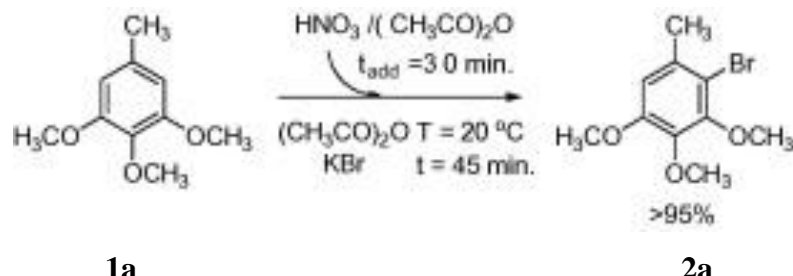


Figure 1: Scheme of synthesis of 2-bromo-3,4,5-trimethoxytoluene

The reaction mixture was then quenched with water and stirred for 30-40 minutes at room temperature. The quenched reaction mixture was then extracted with ethyl ether ( $3 \times 10$  mL). The organics were combined and washed with saturated brine solution, dried over sodium sulphate, filtered, and the solvent was then removed under reduced pressure to achieve 2-bromo-3,4,5-trimethoxytoluene **2a** (colorless – yellowish oil). <sup>1</sup>H NMR spectra were recorded on NMR spectrometer operating at 400 MHz.

### **3.3 Experimental**

#### **3.3.1 Batch reaction**

An ordinary round-bottom flask with three bottlenecks was fitted with a temperature probe and Raman probe while third opening was used for reagent addition to the vessel. The bottleneck holding the optical probe was properly wrapped with Parafilm to avoid any contamination. The reagents were added quickly (<10 sec) according to the scheme given in Table 3.1 and the vessel was resealed afterwards to avoid any contamination. Contrary to the protocol<sup>51</sup>, the concentration of the substrate was doubled in the experiments than the stoichiometric requirements, while volume of acetic anhydride was kept constant. This initiative was taken in order to investigate the progress of the reaction with a lower volume of the solvent because the substrate handling was always easier than the solvent in an industrial environment. The reaction vessel was then placed in a thermostat bath provided with a stirring arrangement using a Teflon coated stirring bar. The laser beam from the Raman instrument was focused on the reaction mixture. The Raman probe and the reaction vessel were kept in fixed positions during the experiments. The distance between probe tip and reaction mixture was adjusted using laser focusing to minimize baseline noise. The reaction monitoring was done in the dark to avoid any fluorescence interference from ordinary light.

Table 3.1: Scheme of experiments carried out in batch conditions

Reaction	Substrate Conc. (M)	3,4,5- trimethoxytoluene (mg)	KBr (mg)	Acetic Anhydride (mL)	HNO <sub>3</sub> (mL)
1	0.15	0.5467	0.357	20	0.22
2	0.3	1.0933	0.714	20	0.44
3	0.6	2.2322	1.4285	20	0.88

#### **3.3.2 Multi jet oscillating disk (MJOD) milli reactor**

The MJOD Milli Reactor used in the current study was developed in our laboratory. The detailed description can be found in the literature<sup>52</sup>. The reactor was a tubular reactor; made of stainless

steel, 150 cm in length with 13 cm outer diameter. The effective volume of the reactor was found to be  $79 \pm 2$  mL. The reactor was comprised of one chamber fitted with an oscillator in the longitudinal direction. The oscillator was fitted with a large number of perforated discs and was powered with a motor which sustained its pulsating to and fro movement in the chamber to maintain good mixing conditions. An annular reaction space was created between the outer surface of the oscillator and the inner surface of the chamber.

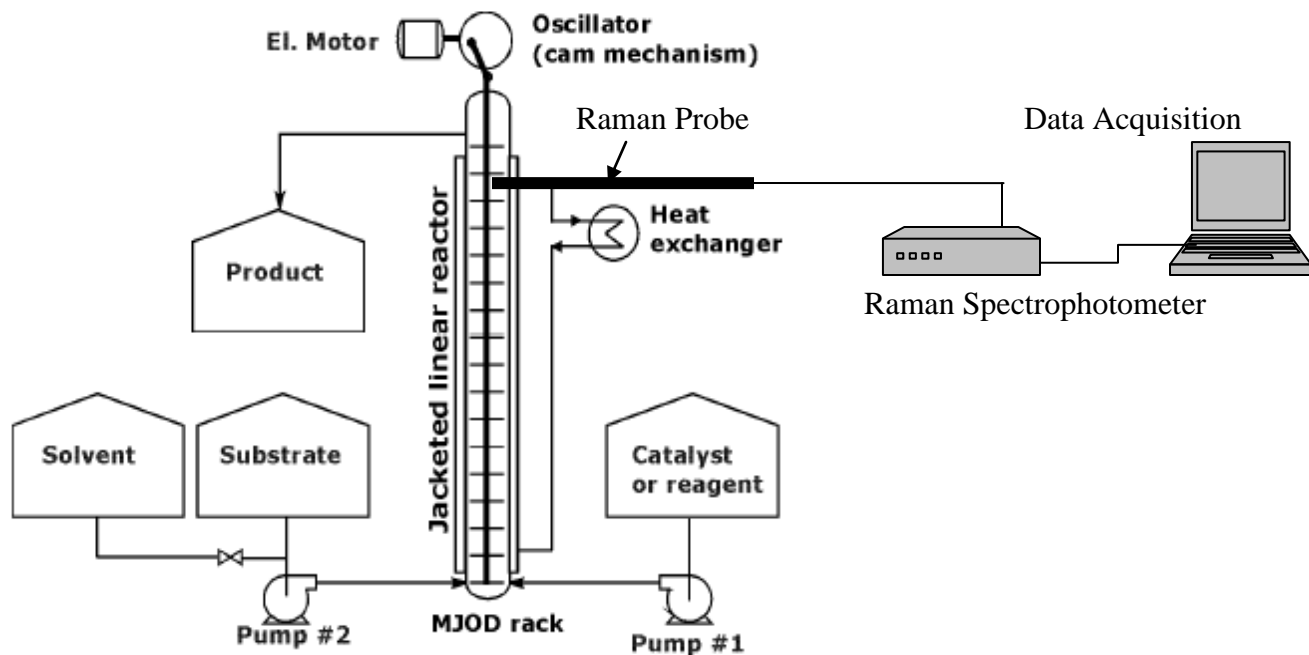


Figure 2: A schematic layout of MJOD Reactor system integrated with Raman system

The reactants were injected into the reaction chamber (scheme given in Table 3.2) by means of pumps through the inlets at the bottom of reactor. Acetic anhydride and nitric acid solution was pumped using lab scale Q Pump (Model QG20-2, Fluid Metering Inc, USA) at a flow rate of  $0.44 \text{ mL min}^{-1}$  whereas mixture of substrate, KBr, acetic anhydride and air was pumped using an FMI lab pump (Model QBG, Fluid Metering Inc, USA) at a flow rate of  $1.58 \text{ mL min}^{-1}$ . The air was introduced to carry over solids (substrate and KBr) in the mixture using a syringe pump (Model KDS-100-CE, Kd Scientific, USA) at a flow rate of  $0.26 \text{ mL min}^{-1}$ . The oscillator pulsation was kept constant at 106 rpm. The temperature was kept constant to room temperature by means of a water circulation assembly (HAAKE F3 FISONS). The Raman probe was positioned through a tailored made hole in the production line coming from the reactor for

spectral recording. The product was withdrawn from an outlet of the reactor into a cylinder and quenched with water under continuous stirring conditions. The higher concentration as compared to the batch reactions was employed due to the volume of the reactor. However, the ration between the substrate and the solvent was kept constant.

Table 3.2: Scheme of bromination of 3,4,5-trimethoxytoluene in MJOD Milli Reactor

Reaction	Substrate Conc. (M)	3,4,5- trimethoxytoluene (mg)	KBr (mg)	Acetic Anhydride (mL)	HNO <sub>3</sub> (mL)
1	0.15	1.096	0.952	40	0.6
2	0.3	2.1919	1.904	40	1.2
3	0.6	4.3838	3.808	40	2.4

### 3.4 Raman Spectroscopy

Raman spectra were recorded using Raman Rxn1 instrument from Kaiser Optical Systems, Inc. USA. It was equipped with a charge-coupled device detector for the batch and continuous reaction monitoring. The spectrometer was fitted with an 18 inch immersion probe (0.5 inch diameter) on a Kaiser MR probe head connected to the base unit via a fiber-optic cable. The Raman excitation source was an Invictus 785 nm diode laser (Kaiser Optical Systems, Inc. USA) with a power of 400 mW. The laser power at the sample used was over 100 mW. Reaction monitoring was carried out at following acquisition settings: 100ms exposure time, 6 accumulations, intensity calibration on, dark subtract on, and an acquisition interval of 0 sec with 1 count. Five spectra per minute were recorded using these settings.

The effect of system disturbances (pump and oscillator) on the Raman signal was studied using acetic anhydride in the reactor. Acetic anhydride was pumped at different flow rates (2, 3 and 10 mL min<sup>-1</sup>) and at different oscillator settings (50, 78 and 106 rpm). The spectra were recorded on afore mentioned Raman instrumental setting.

### 3.5 Data acquisition and analysis

HoloGRAMS (version 4.0, Kaiser Optical Systems) was used to control the spectrophotometer. The recorded spectra were exported using HoloReact (version 2, Kaiser Optical Systems) to

Matlab 7.4 (Mathworks, Natick, MA). The Raman spectra for each reaction (Batch + Reactor) were combined into one data matrix;  $A_{m \times n}$ , with ‘m’ reaction spectra (rows) and ‘n’ Raman frequencies (columns) ranging from -92 to 3453  $\text{cm}^{-1}$ . The Sirius (version 8.0, PRS-Norway) was used for statistical analysis. The raw spectral data was subjected to the second order differentiation for preprocessing before any analysis.

## **Results and Discussion**

### **4.1 Disturbance diagnosis for MJOD reactor**

The MJOD reactor system used in this study had two settings that could be manipulated and hence, two possible process disturbances; the oscillator and two feeding pumps. The oscillator was responsible for the vigorous mixing of the reactants inside the reactor while the pumps were responsible for the smooth injection of reactants into the reactor. Any possible fluctuation in any of these process variables could lead to process malfunctioning in terms of lower product quality or system breakdown. Thus, it was of prime interest to investigate their potential to be considered as process disturbances. Both the disturbances were evaluated using different instrumental settings to determine their impact on the system. A one component system, pure acetic anhydride was used for this study in order to avoid any contribution from chemical change during the process.

#### **4.1.1 Oscillator effect**

The oscillator was operated at three different settings (50, 78 and 106 rpm) in order to monitor its effect on the process whereas pump speed was kept constant to avoid any contribution. The PC model of the second order differentiated spectral data showed that first two PCs explained 30% variance. The Hotelling test statistics  $T^2$  was applied to define a 95% tolerance region in order to ensure control for the recorder spectra. The score plot (Fig. 4.1) showed that there was no systematic relationship among the spectra of three oscillator settings implying that the system was independent of oscillation speed. This fact was also confirmed by the plot showing the raw spectra for this experiment (Appendix.1, Fig. A1). The score values for these settings were randomly distributed whereas some of the score values were found near or outside the  $T^2$  ellipse. These values belonged to the spectra which were recorded either at the start or at the end of any experiment. This situation arose due to the adjustment of measurement system. The oscillator was operated at the maximum oscillation speed (106rpm) throughout the following experiments in order to maintain good mixing conditions inside the reactor.

#### **4.1.2 Pump effect**

The pump was operated at three different settings (2, 3 and 10 mL/min) while the oscillator was operated at constant speed 106rpm. The score plot (Fig. 4.2) for first two PCs showed that the spectra belonging to different pump settings were randomly distributed. Only a few scores for the spectra recorded at the start or at the end of the experiment were present outside the ellipse due to the initial adjustment of the measurement system. However, the raw Raman data for this plot revealed that there was some noisy overlapping among different bands in the raw spectra (Appendix.1, Fig. A2). This could be attributed due to the presence of cosmic rays<sup>34</sup>.

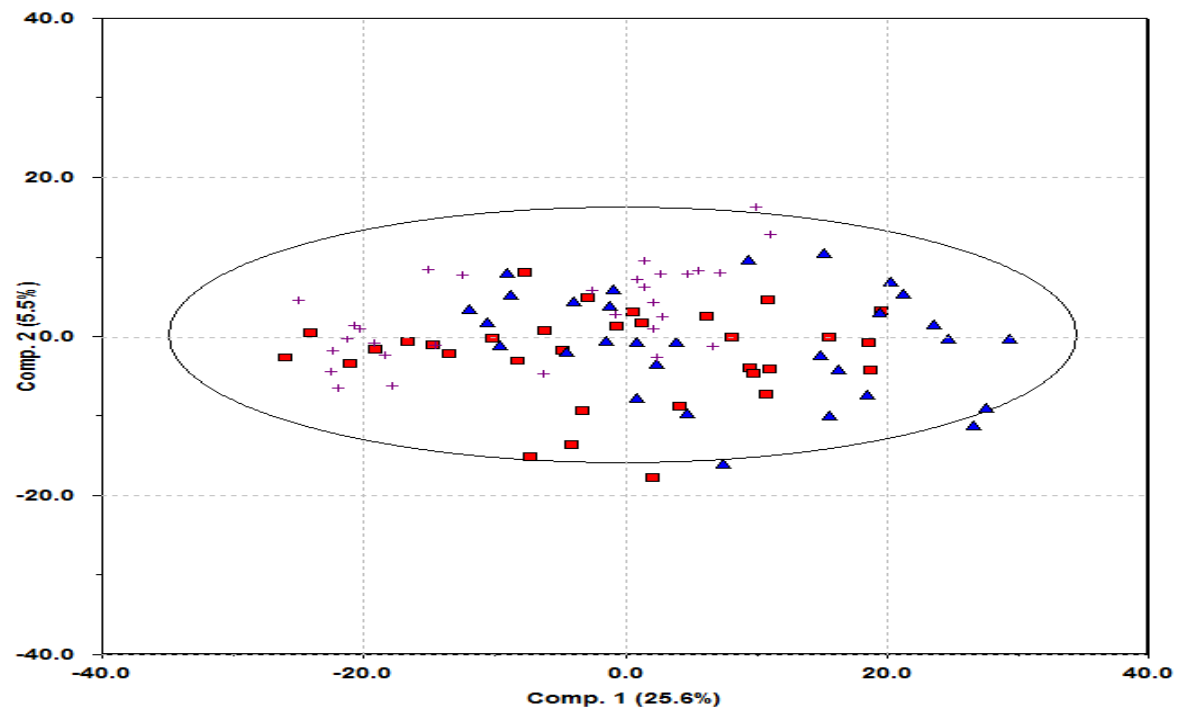


**Figure 4.1:** Effect of various oscillator settings on the process;  $\Delta=50\text{rpm}$ ,  $\square=78\text{rpm}$ ,  $+$  =  $106\text{rpm}$

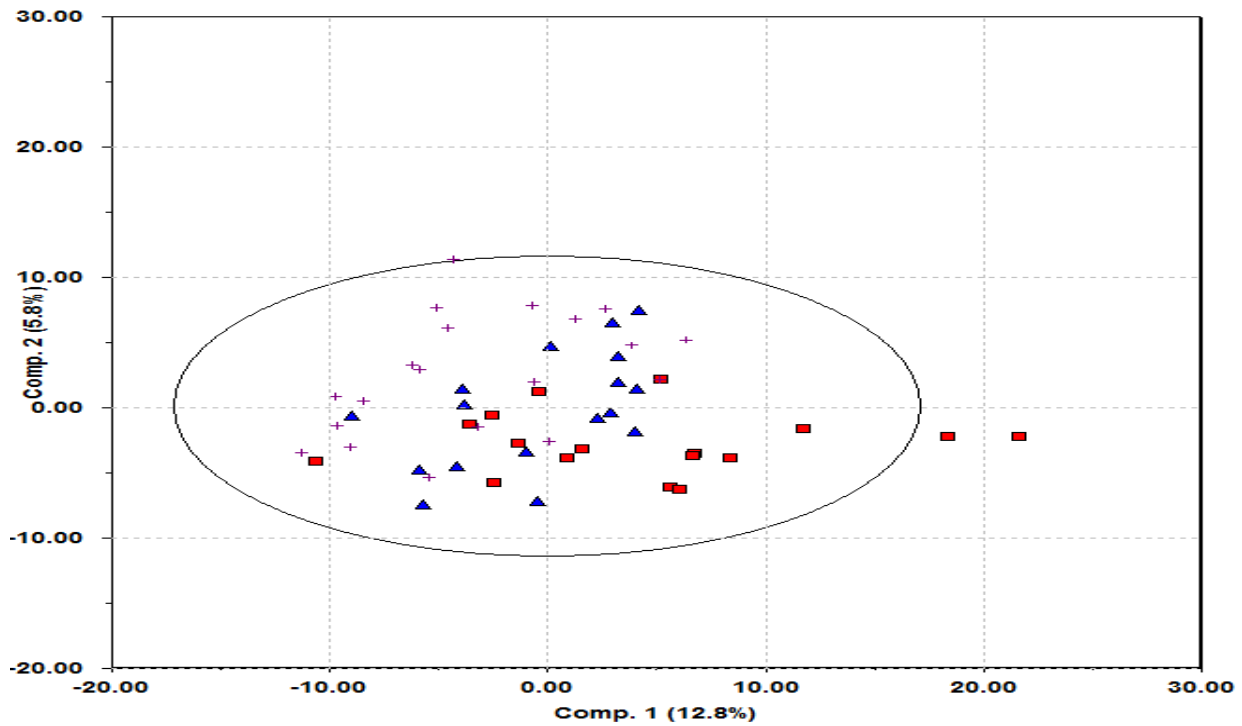


**Figure 2:** Effect of pump settings on the process;  $\Delta = 2\text{mL/min}$ ,  $\square = 3\text{mL/min}$ ,  $+$  =  $10\text{mL/min}$

## 4.2 Raman Spectra

The synthesis of 2-bromo-3,4,5-trimethoxytoluene was carried out under the batch conditions and in the MJOD reactor according to the schemes as given (Table 3.1 and 3.2). The spectra of the solvent (acetic anhydride), substrate (3,4,5-trimethoxytoluene) and product (2-bromo-3,4,5-trimethoxytoluene) are given in Fig. 4.3. It is evident that the spectra experienced some band overlapping throughout most of the spectral region. The spectrum of acetic anhydride was characteristic at  $675\text{ cm}^{-1}$  which was assigned to C=O bond vibration<sup>53</sup>. This intense peak was absent in all the other spectra, making it the distinguished spectral region for acetic anhydride. The spectra for substrate and product were similar, but differed in terms of intensity. The bands in the spectra of product were slightly shifted to higher wave numbers compared to the substrate spectra. The substrate was characterized by two spectral regions;  $990\text{-}1020\text{ cm}^{-1}$  which was assigned to trisubstituted benzene ring and  $1025\text{-}1060\text{ cm}^{-1}$  which was assigned to the ring vibration for ortho-disubstituted benzene. These regions were noticed to be very vibrant during several runs both in the batch and in the MJOD reactor. Both these spectral regions were also found for the product. However, the intensity was as about one third of the substrate's intensity. The product was characterized due to the presence of CBr stretching<sup>54</sup> at  $550\text{ cm}^{-1}$ .

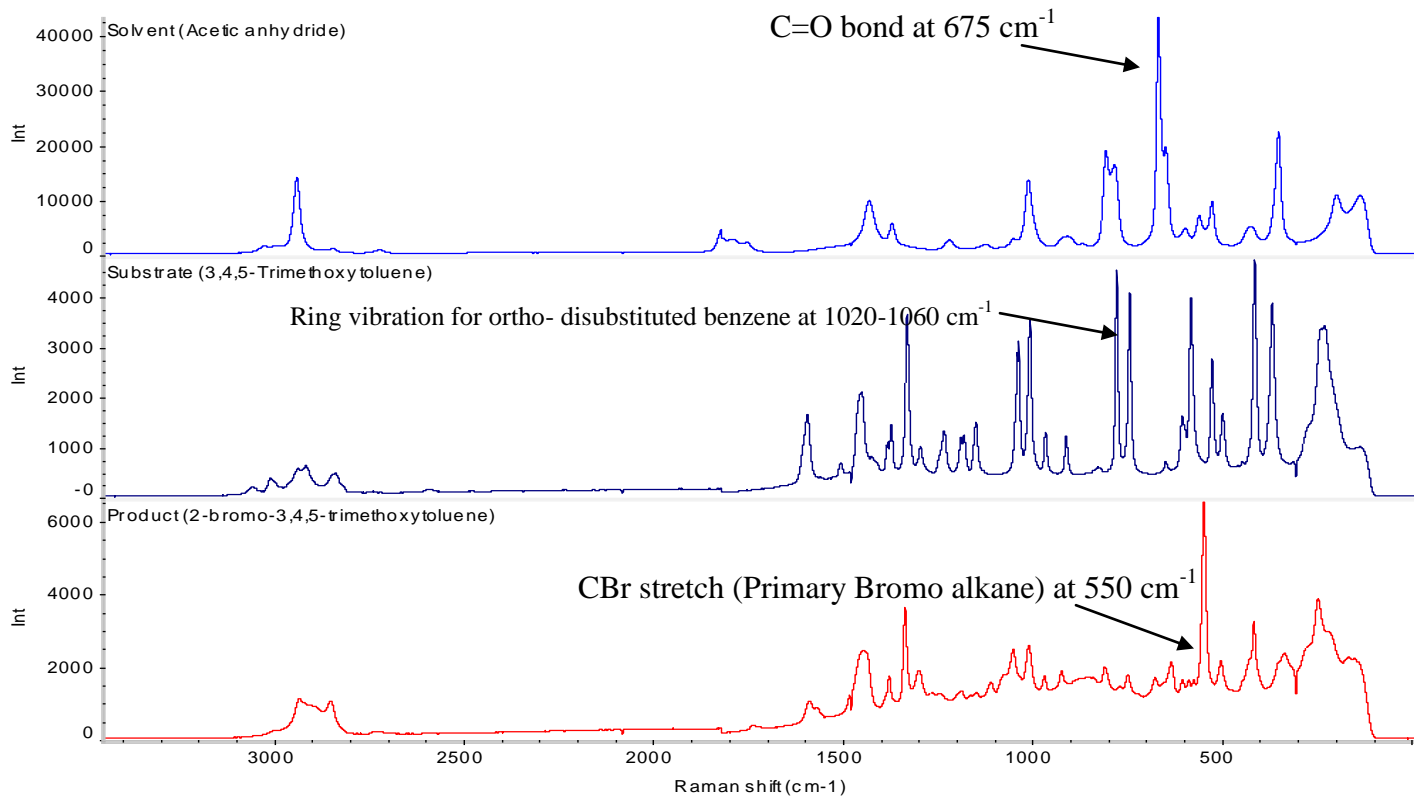


**Figure 4.3:** Pure spectra of the solvent, substrate and the product (From top to bottom)

### 4.3 Monitoring the Synthesis of 2-Bromo-3,4,5-Trimethoxytoluene

#### 4.3.1 Reaction 1

##### 4.3.1.1 Batch reaction

The raw Raman data set for Reaction 1 under batch conditions is presented in Fig.4.4. The important spectral regions were identified as  $550$  and  $1050\text{ cm}^{-1}$ . The frequency  $550\text{ cm}^{-1}$  was assigned to CBr stretching and  $1050\text{ cm}^{-1}$  was responsible for ortho substitution of the substrate. The intensity plot for both these frequencies showed some kind of repeated reactions at regular time intervals during the reaction (Fig. 4.5). It was clear that the substitution of Br increased during the first 15 minutes of the reaction and then suddenly decreased. Apparently, the product formation continued to increase besides the decrease in the intensity at  $1050\text{ cm}^{-1}$ . However, normal behavior was again witnessed during the last part of the reaction.

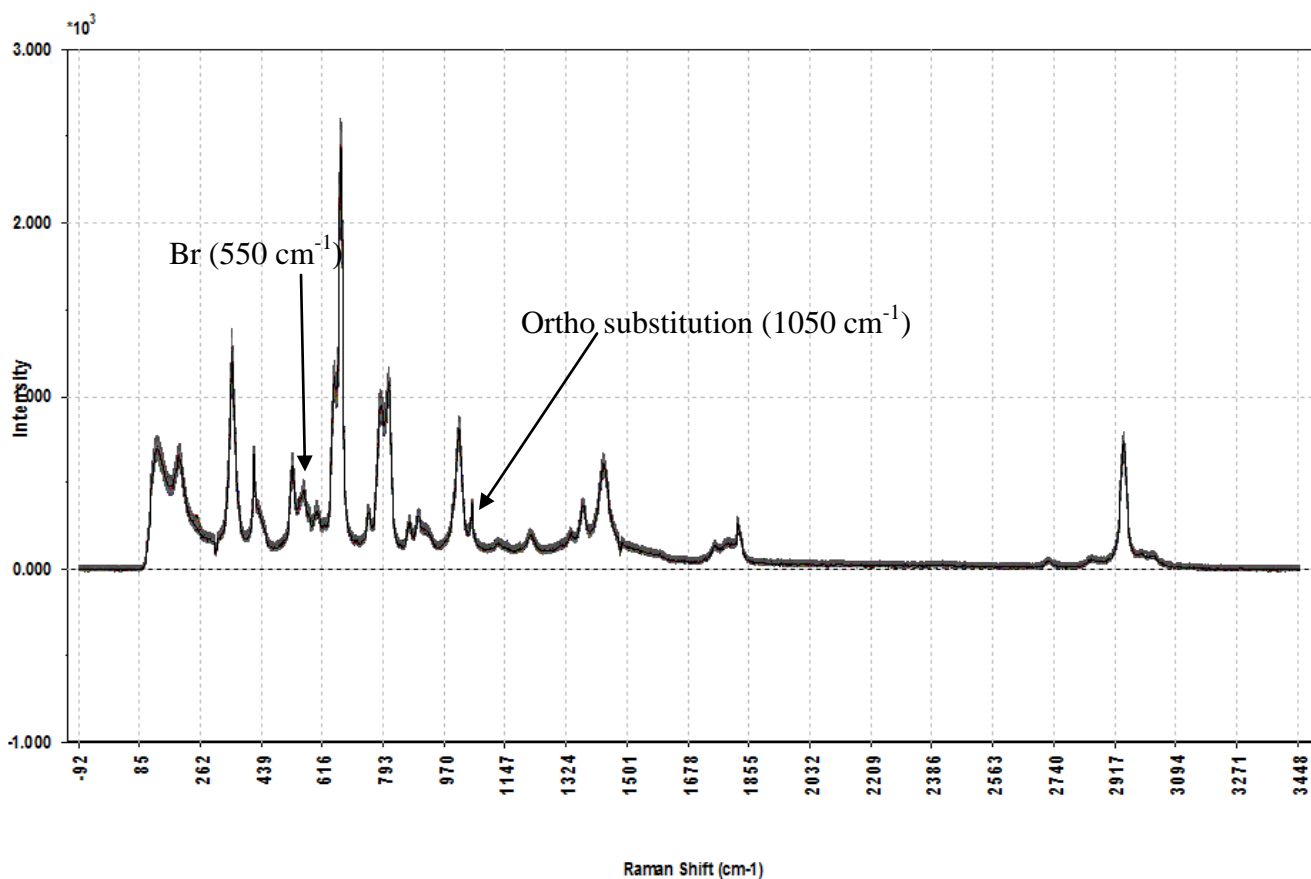


**Figure 4.4:** The raw Raman data for Reaction 1 under batch conditions

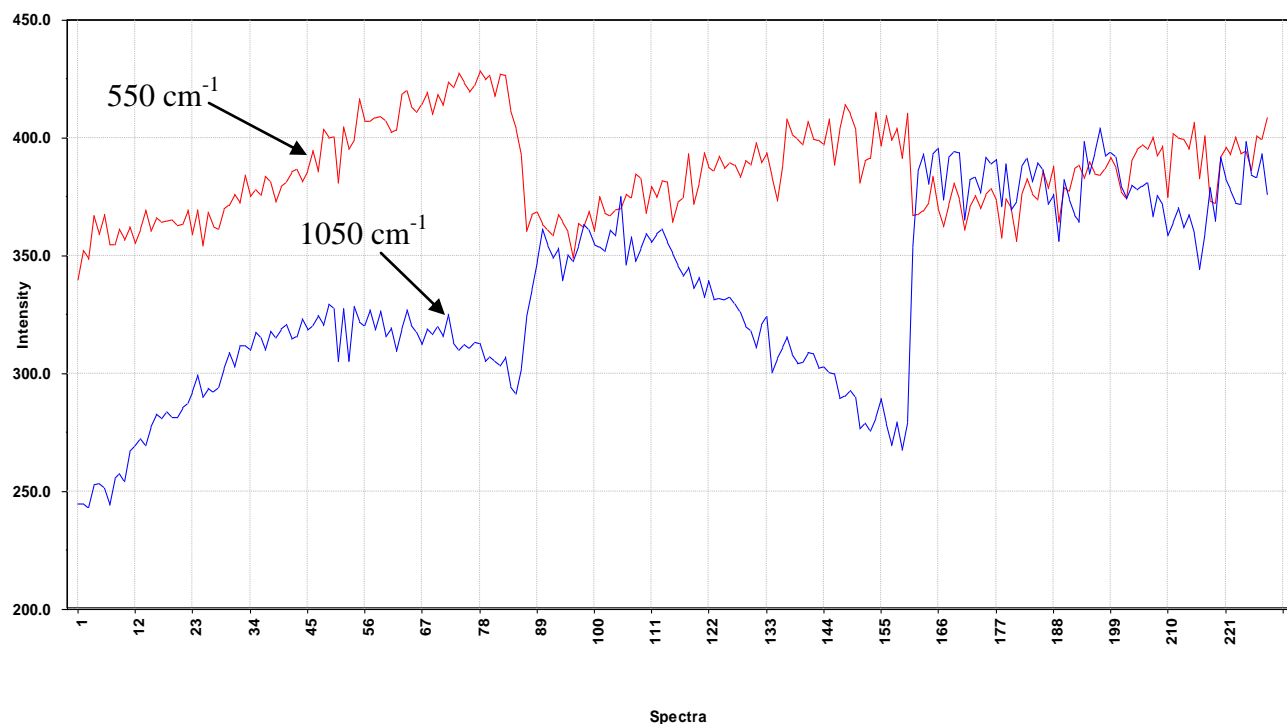


**Figure 4.5:** Intensity plot for two Raman frequencies ( $550$  and  $1050\text{ cm}^{-1}$ ) for Reaction 1 under the batch conditions

This shift in the intensity at  $1050\text{ cm}^{-1}$  could be justified with the slight increase in temperature of the reaction mixture. It was noticed that temperature of the reaction mixture initially increased by  $5^\circ\text{C}$  which was then counteracted to room temperature. The synthesis protocol of the product suggested that bromination of the substrate should be carried out at  $20^\circ\text{C}^{52}$ . Thus, a slight shift in the temperature could be responsible for the repeated pattern in the intensity plot as reported<sup>10</sup>.

The score plot of first two PCs also exhibited similar information (Fig. 4.6). The reaction profile seemed to be evolutionary as a function of time however some overlapping among the spectra was also observed. The respective reaction profile using score values against the reaction time clearly validated aforementioned facts (Fig. 4.7). The respective biplot explained the distribution of spectra on the basis of Raman frequencies (Appendix 1, Fig. A3). This plot showed Raman band around  $650$ - $680\text{ cm}^{-1}$  which was characteristic for the solvent. The start and end of the reaction was distinguished on the basis of Raman frequencies  $1050$  and  $550\text{ cm}^{-1}$  which represented the formation of the product and ortho-substitution in the substrate respectively. The respective loading plot was also given to explain the contribution of the relevant Raman frequencies (Appendix 1, Fig. A4).

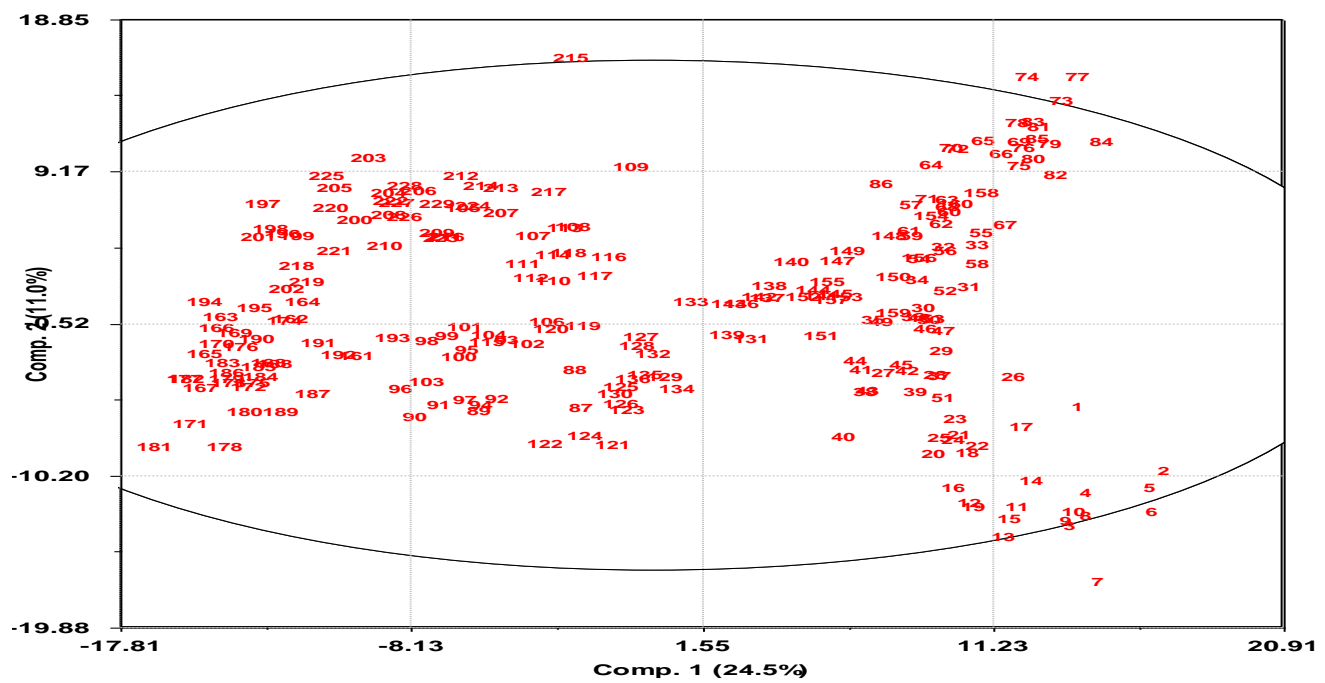


**Figure 4.6:** Score plot for spectra based on first two PCs for Reaction 1 under batch conditions

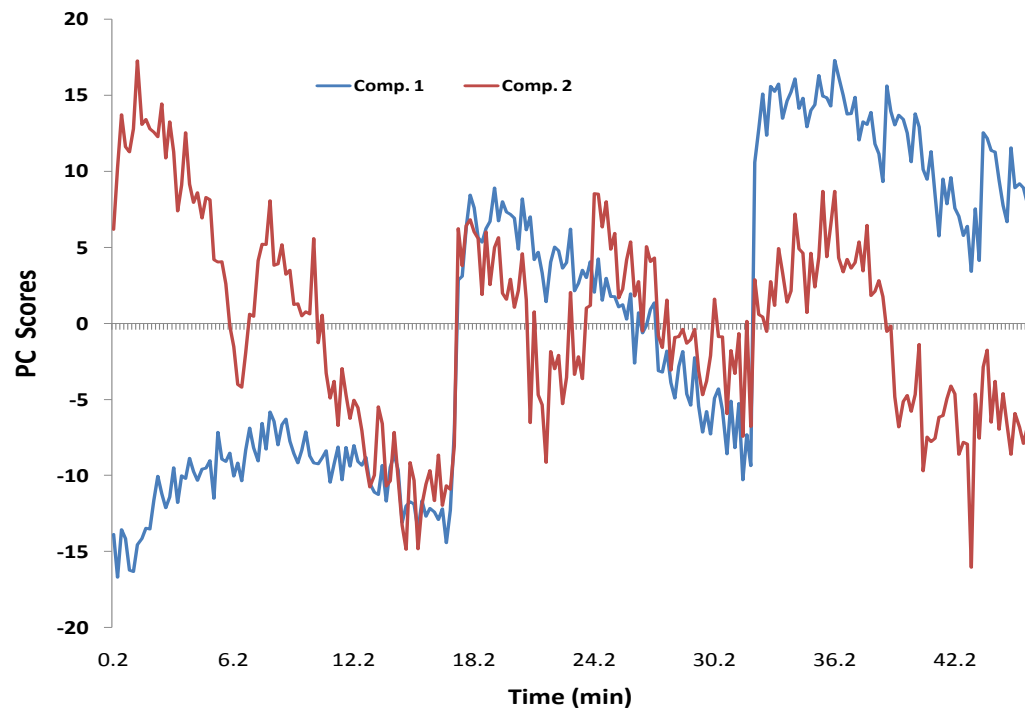


**Figure 4.7:** Reaction profile based on score values of first two PCs for Reaction 1 under batch conditions

#### 4.3.1.2 MJOD reaction

The raw Raman data set for two runs of Reaction 1 in the reactor is presented in Fig. 4.8. It was evident that the spectra observed a diverse behavior during the two runs for Reaction 1 in the reactor. In order to investigate this pattern, the score plot based on the first two PCs was obtained from the preprocessed spectral data (Fig. 4.9). The score plot demonstrated that one part of the spectra from the first run in reactor ( $\Delta$ ) was entirely different from the rest of the spectra and was grouped apart. This discrimination was observed due to the breakage of one of the feed pumps during the first run. The measurement system detected this disturbance and grouped the affected spectra separately. For this run, overall conversion of the substrate was found to be 89% whereas yield of the product was only 49% (Appendix 1, Table A.5). The second run (+) observed an 86% conversion and 60% yield of the product. The respective biplot discriminated first part of the spectra for first run from other spectra on the basis of Raman frequencies ranging from 650-680  $\text{cm}^{-1}$  (Fig. 4.10). Thus, only acetic anhydride was fed into the reactor during the first part of the first run because the feeding pump was broken due to the clogging caused by the solids (substrate and KBr).

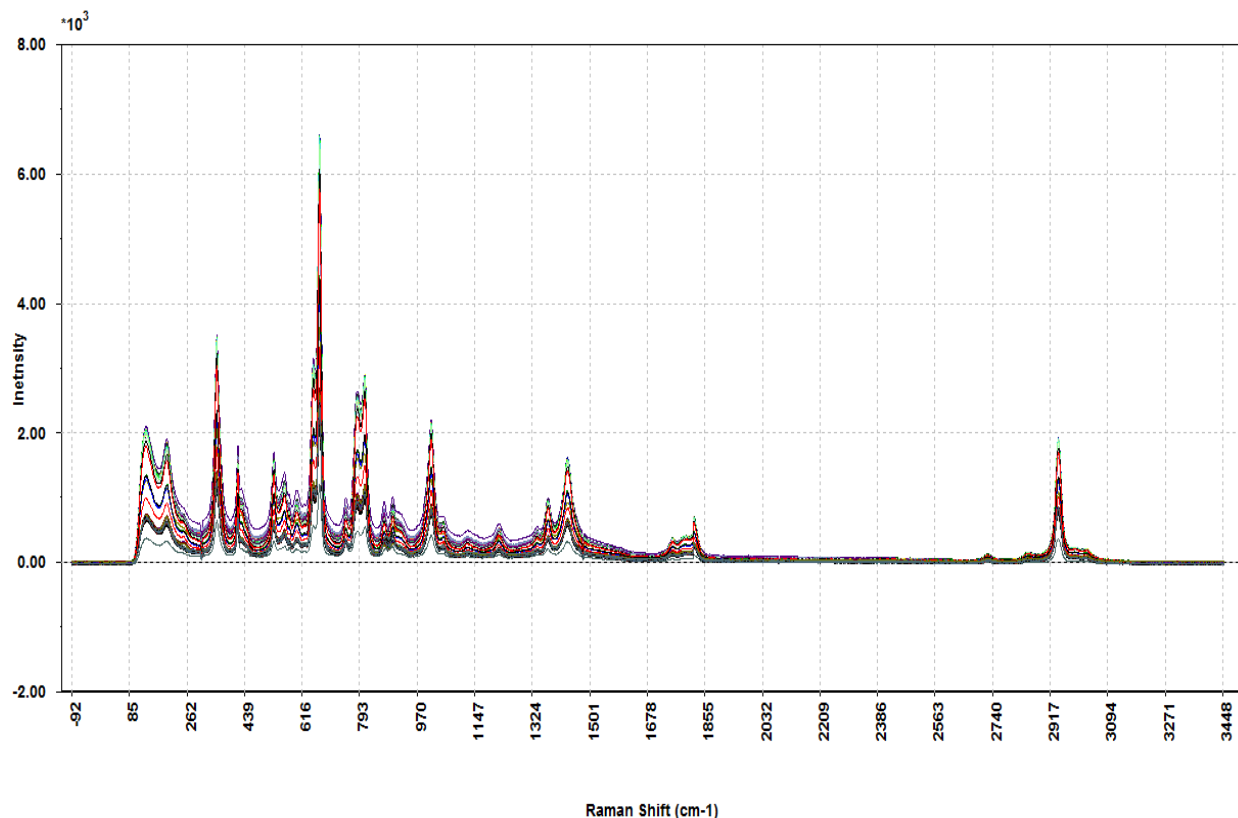


**Figure 4.8:** The raw Raman data for two runs in the reactor for Reaction 1

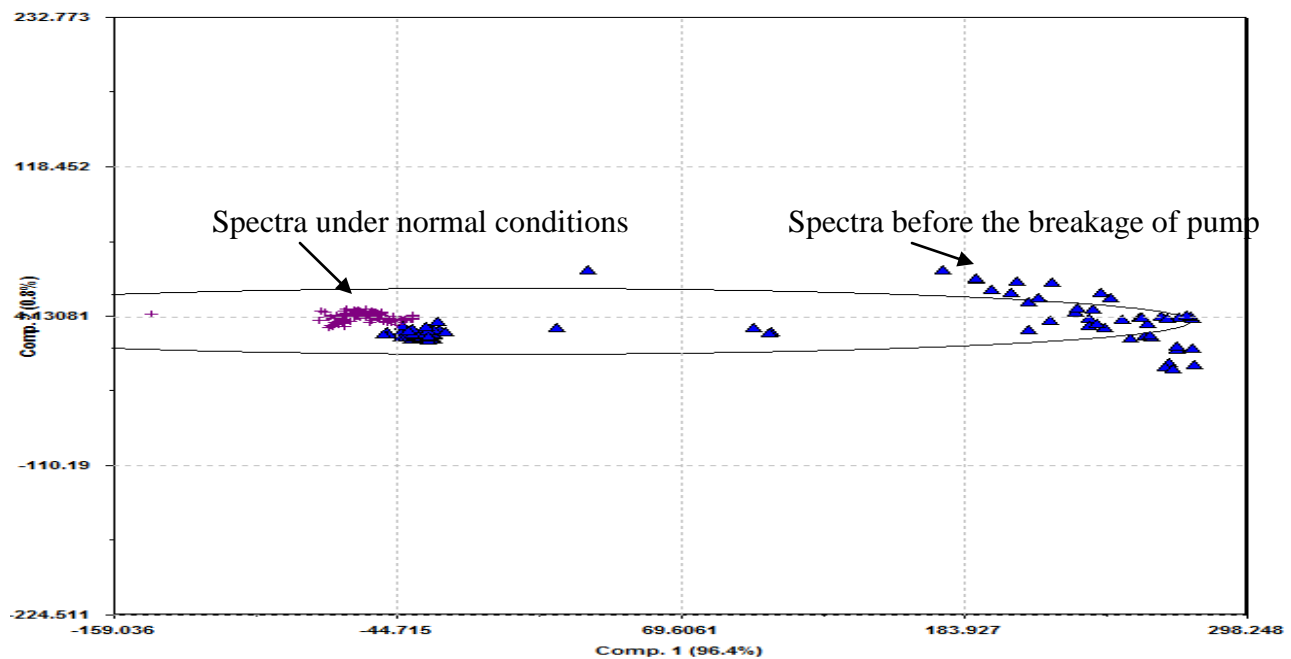


**Figure 4.9:** The score plot for two runs; first ( $\Delta$ ) and second (+), in the reactor for Reaction

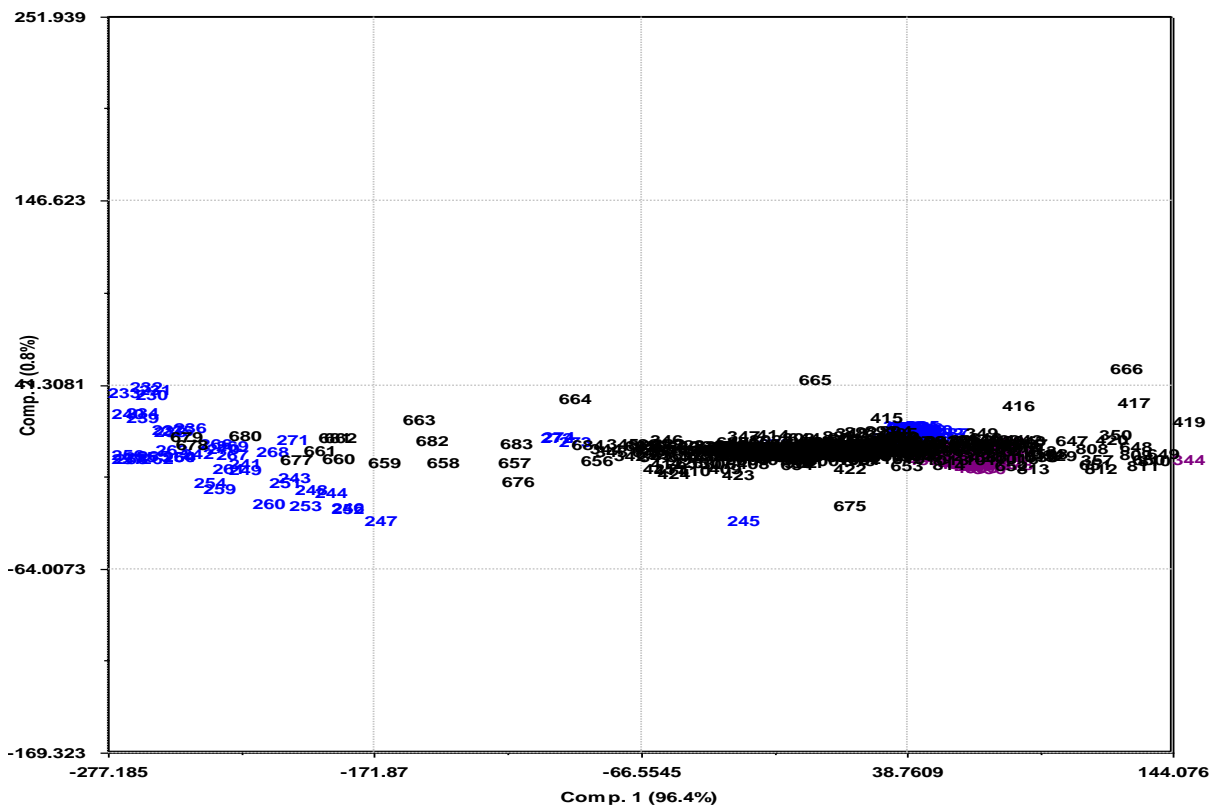


**Figure 4.10:** Biplot for the two runs in the reactor for Reaction 1

The feeding of only acetic anhydride to the reactor before the breakage of the pump was also verified by the respective intensity plot of spectra at  $894\text{ cm}^{-1}$  (Fig. 4.11). It showed that the intensity at  $894\text{ cm}^{-1}$  increased initially and then started decreasing until the pump stopped working. It disclosed that initially only acetic anhydride was pumped into the reactor meanwhile the solids started building up around the piston in the pump until the pump.

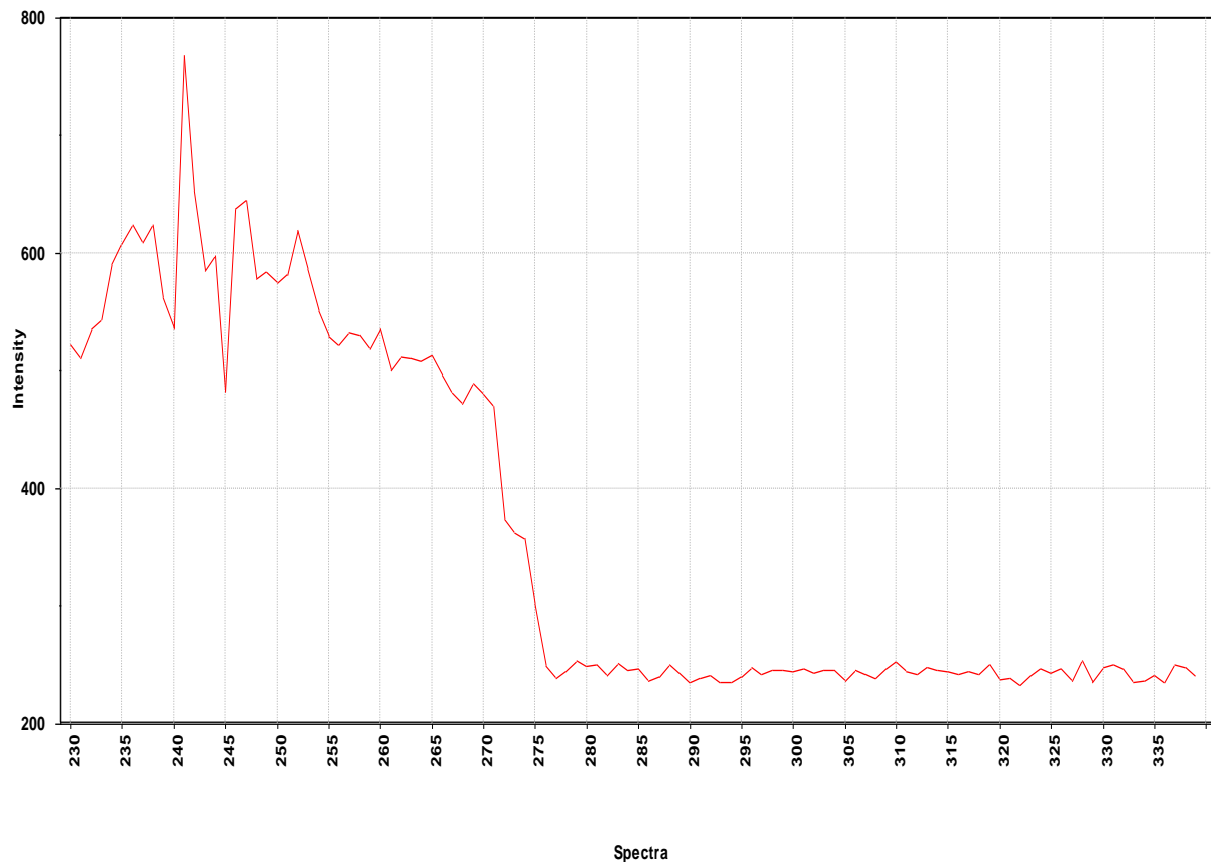


**Figure 4.11:** Intensity plot for the spectra of first run in the reactor for Reaction 1 at  $894\text{cm}^{-1}$

### 4.3.2 Reaction 2

#### 4.3.2.1 Batch reaction

The raw Raman data for this reaction is presented in Fig. 4.12. The profile of batch reaction followed an evolutionary behavior over the course of reaction as given by the relevant score plot (Fig. 4.13). At the start of the reaction, the measurement system took some time to adjust and then reaction proceeded in the forward direction. The two component PC model explained almost 63% of the variance in the spectral data.

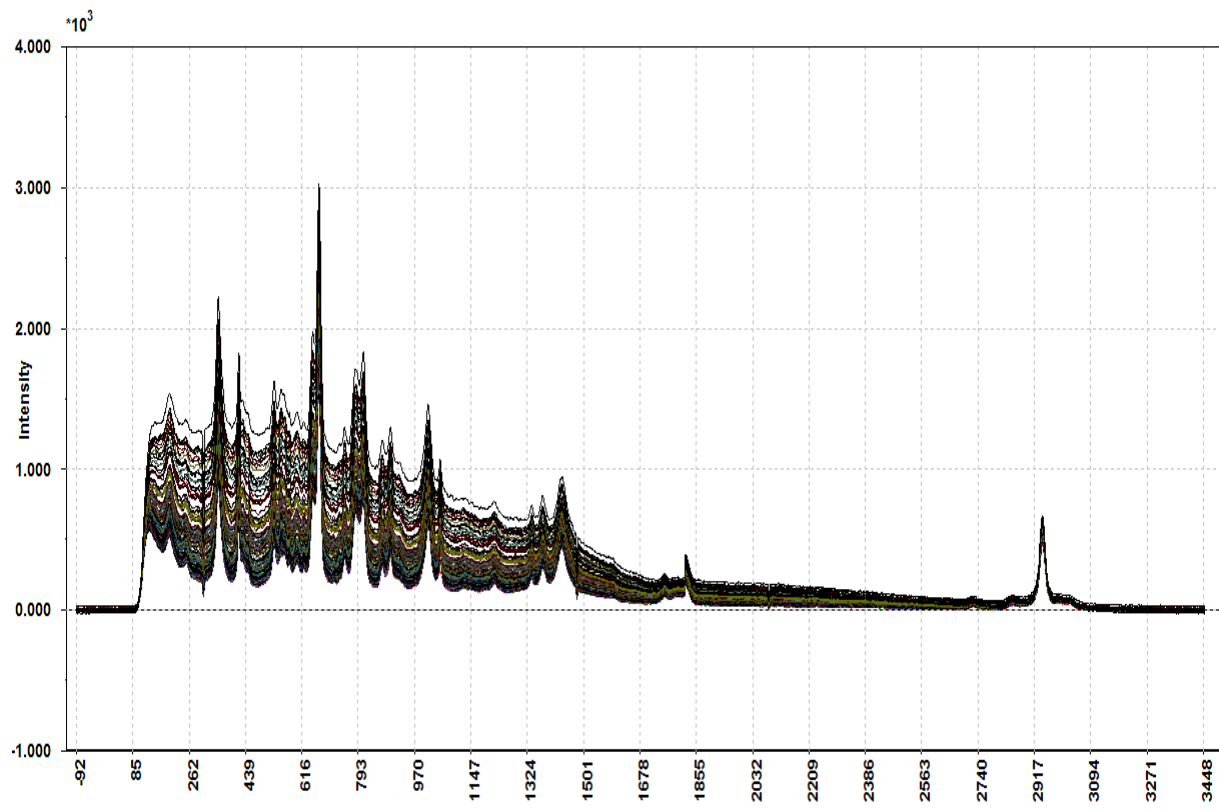


**Figure 4.12:** Raw Raman data for Reaction 2 under batch conditions

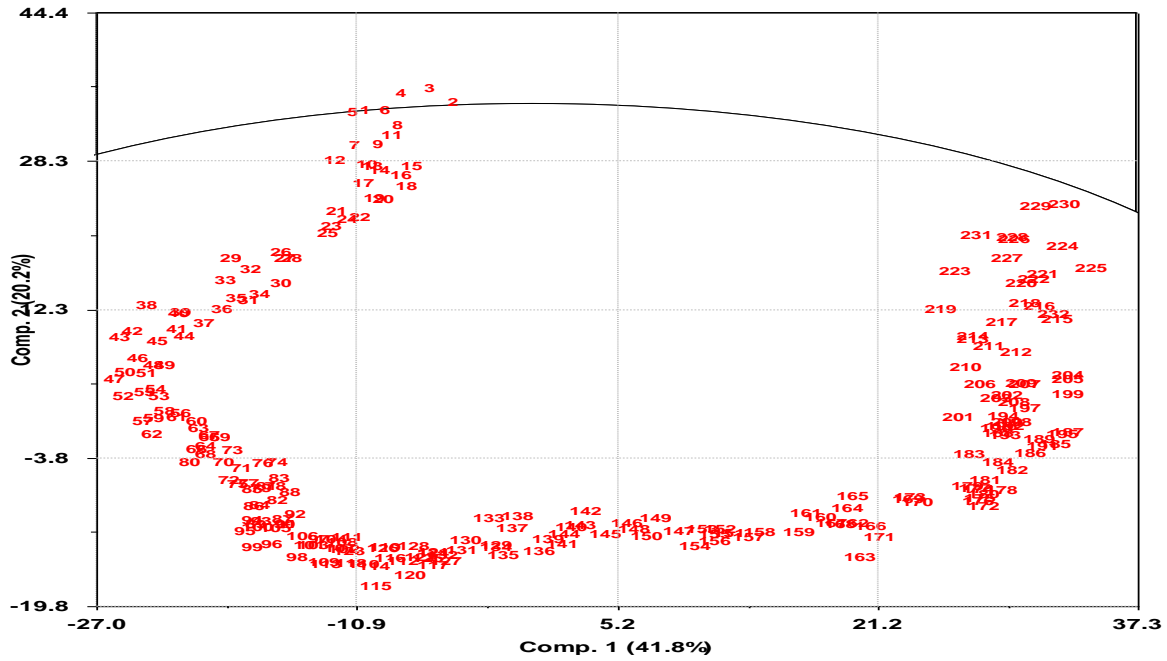


**Figure 4.13:** Score plot based on the first two PCs for Reaction 2 under batch condition

The proceeding of the reaction was also profiled by plotting score values against the reaction time (Fig. 4.14). The score trace for the first PC demonstrated the path of the reaction whereas the second PC showed the changes in the reaction mixture in the vessel as a function of time. The first PC score trace initially observed some decreasing trend during the first 8 minutes of the reaction and it increased gradually thereafter. The score trace for the second PC decreased up to 21 minutes and then again started to increase. This might be due to the presence of some unreacted mixture in the vessel.

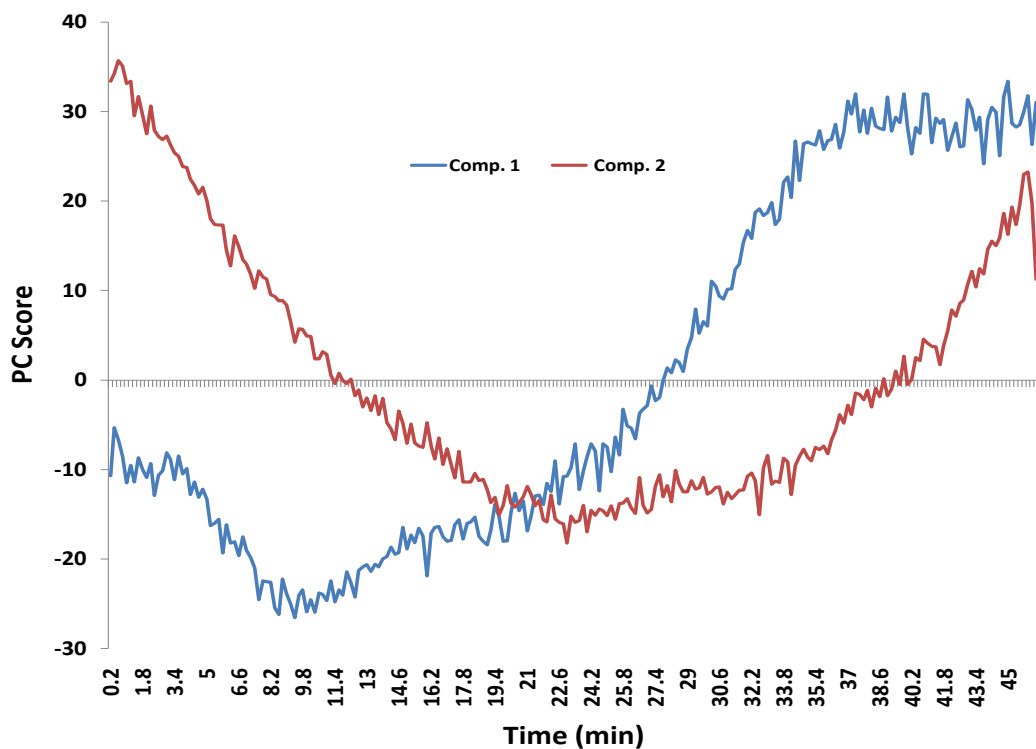


**Figure 4.14:** Reaction profile based on score values of Reaction 2 under batch conditions

The respective biplot explained the distribution of score values in the model (Fig. 4.15). It disclosed that the start of the reaction and the last part of the reaction could be clearly distinguished on the basis of CBr stretching along  $520\text{-}555\text{ cm}^{-1}$  which implied that the product was being formed during this period of reaction. The frequencies from  $1040\text{-}1060\text{ cm}^{-1}$  encompassed all the spectra in the plot confirming the bromination of the substrate. This fact was further verified when the spectra for batch reaction were plotted against Raman intensity for the wave numbers;  $550$  and  $1050\text{ cm}^{-1}$ . It was noticed that the intensity of both these frequencies was continuously increased during the reaction (Figure 4.16). The characteristic frequency range for acetic anhydride ( $650\text{-}680\text{ cm}^{-1}$ ) was obvious in the biplot due its presence in the system throughout the reaction. The dynamics of these characteristic frequencies could be seen in the loading plot as well (Appendix 1, Fig. A6).

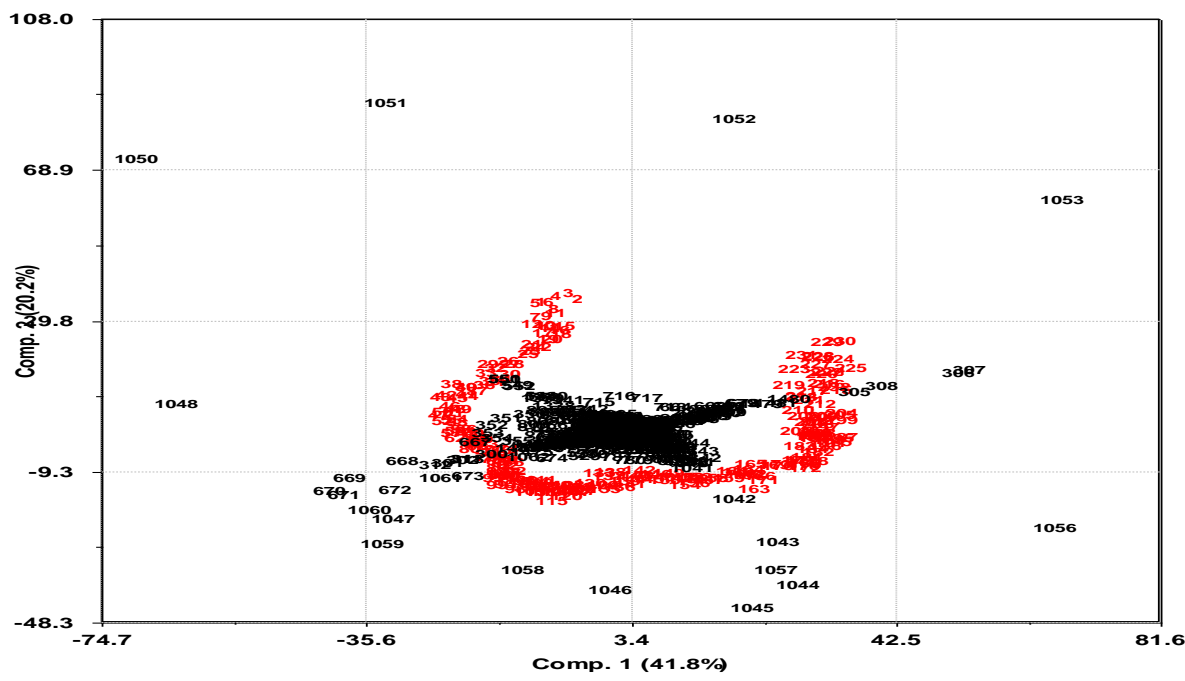


**Figure 4.15:** Biplot for Reaction 2 under batch conditions

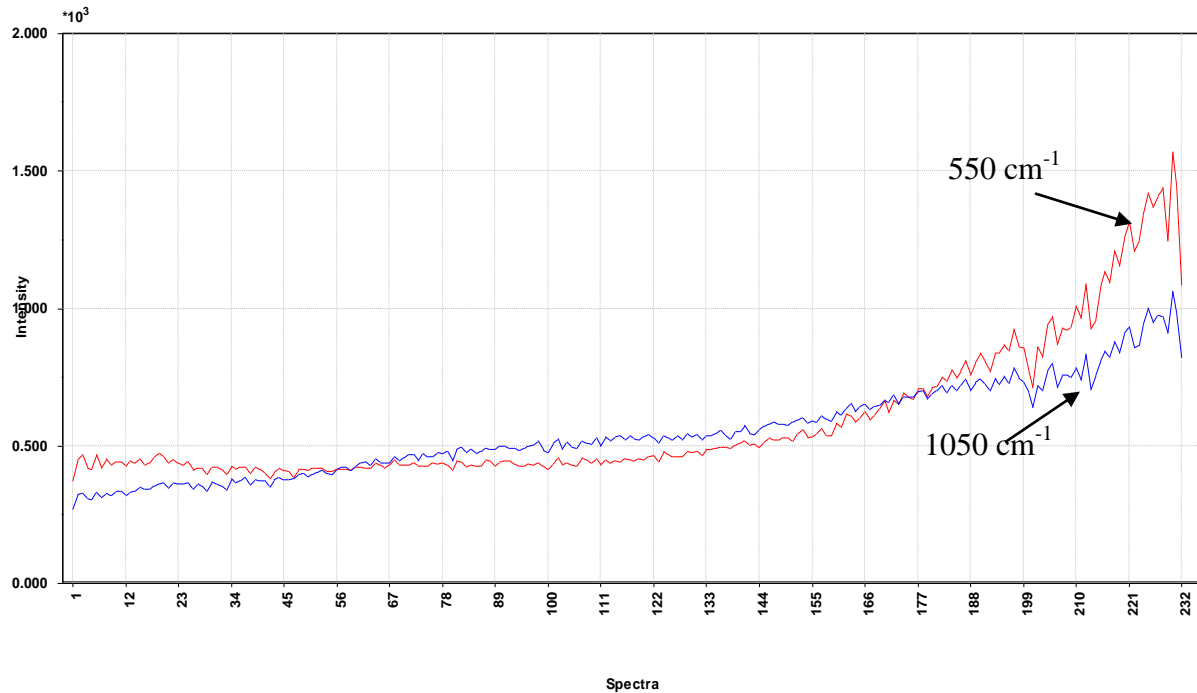


**Figure 4.16:** Intensity plot for Raman frequencies; Red ( $550 \text{ cm}^{-1}$ ) and Blue ( $1050 \text{ cm}^{-1}$ ) for Reaction 1 under batch conditions

#### 4.3.2.2 MJOD reaction

In order to investigate Reaction 2 in the MJOD reactor, three runs under same conditions were performed. Raw Raman data for these runs is presented in Fig. 4.17. The PC model of the preprocessed recorder spectra revealed that the two runs ( $\square$   $\Delta$ ) were in close agreement with each other while one of the run (+) was entirely different (Fig. 4.18). The offline analysis disclosed that the two closely related runs observed a substrate conversion of approximately 95 % ( $\square$ ) and 98% ( $\Delta$ ) respectively, whereas the third run observed only 72% conversion. The Isolated yield for the product was 58, 64 and 34% respectively for these three runs. This information could be a possible explanation for the variation among three runs.

The individual spectral monitoring of third run confirmed that no intense peak was found around  $550\text{cm}^{-1}$  which was the ultimate peak position for the product. Therefore, it was proved that Raman system could discriminate the third run as a chemically different entity from the other two runs and this finding was also confirmed by offline analysis. Thus, the third run was removed from the PC model and a new model was built to analyze the first two similar runs.

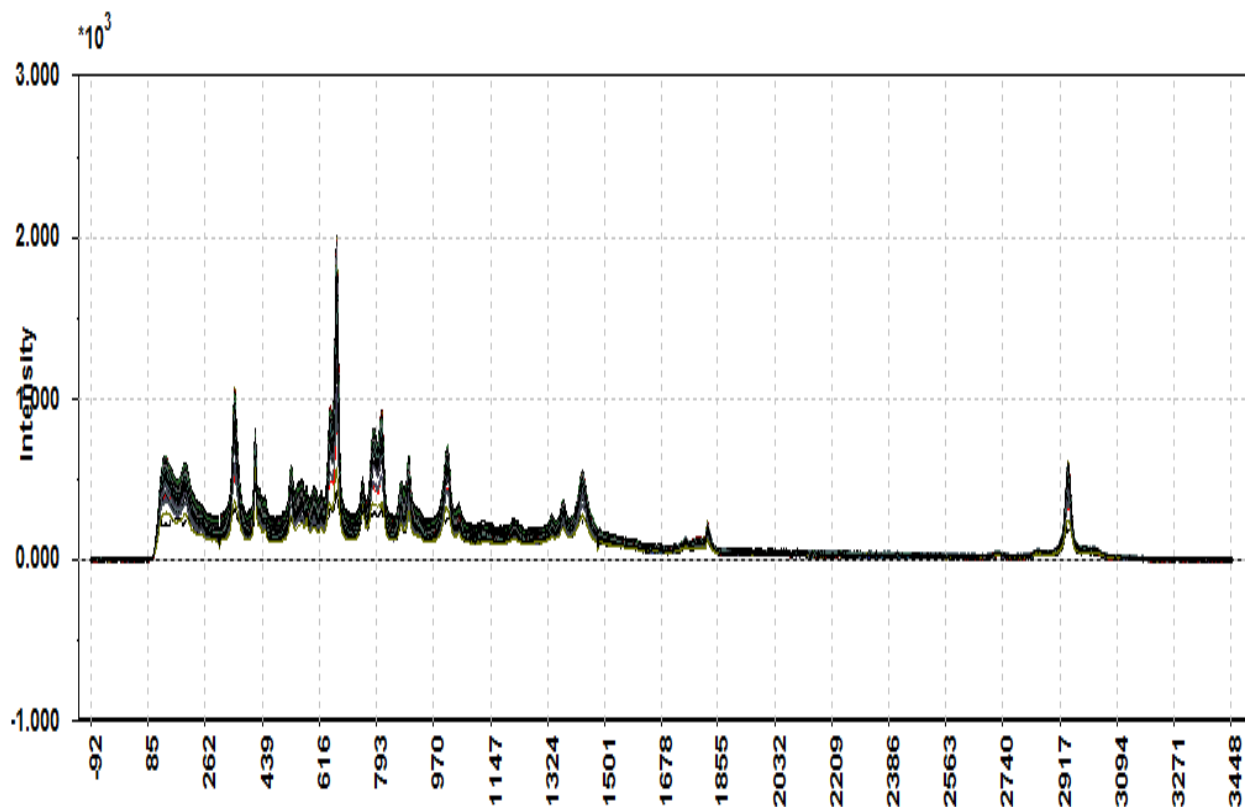


**Figure 4.17:** Raw Raman spectral data of Reaction 2 for three runs in the reactor

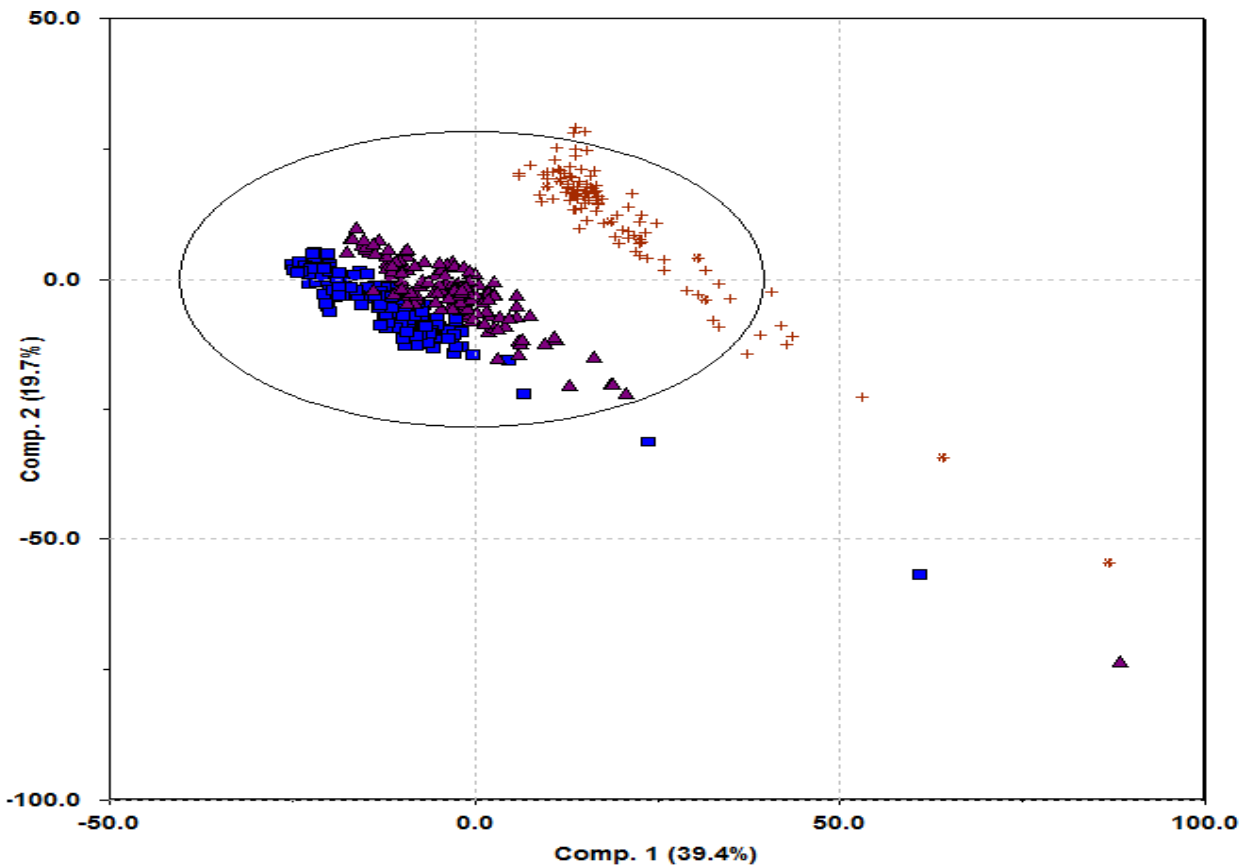


**Figure 4.18:** Score plot for three runs for Reaction 3; first (□), second ( $\Delta$ ) and third (+) in the reactor

The PC model of the two similar runs showed that both the runs were grouped close to each other but were not exactly the same. They were grouped separately in the respective score plot (Fig. 4.19). The possible reason for this grouping was the conversion of the substrate and ultimate yield of the product. The score plot demonstrated some kind of systematic continuity among the spectra. This trend was evident due to the possible back mixing of reaction mixture inside the reactor with the incoming reactants. The biplot described the distribution pattern of the spectra along Raman frequencies (Appendix 1, Fig. A7). The distribution of spectra along first PC was due the presence of acetic anhydride ( $650\text{-}680\text{ cm}^{-1}$ ) while acetic acid ( $890\text{-}895\text{ cm}^{-1}$ ) contributed to the variation along the second PC. This can be further verified by respective loading plot (Appendix 1, Fig. A8).

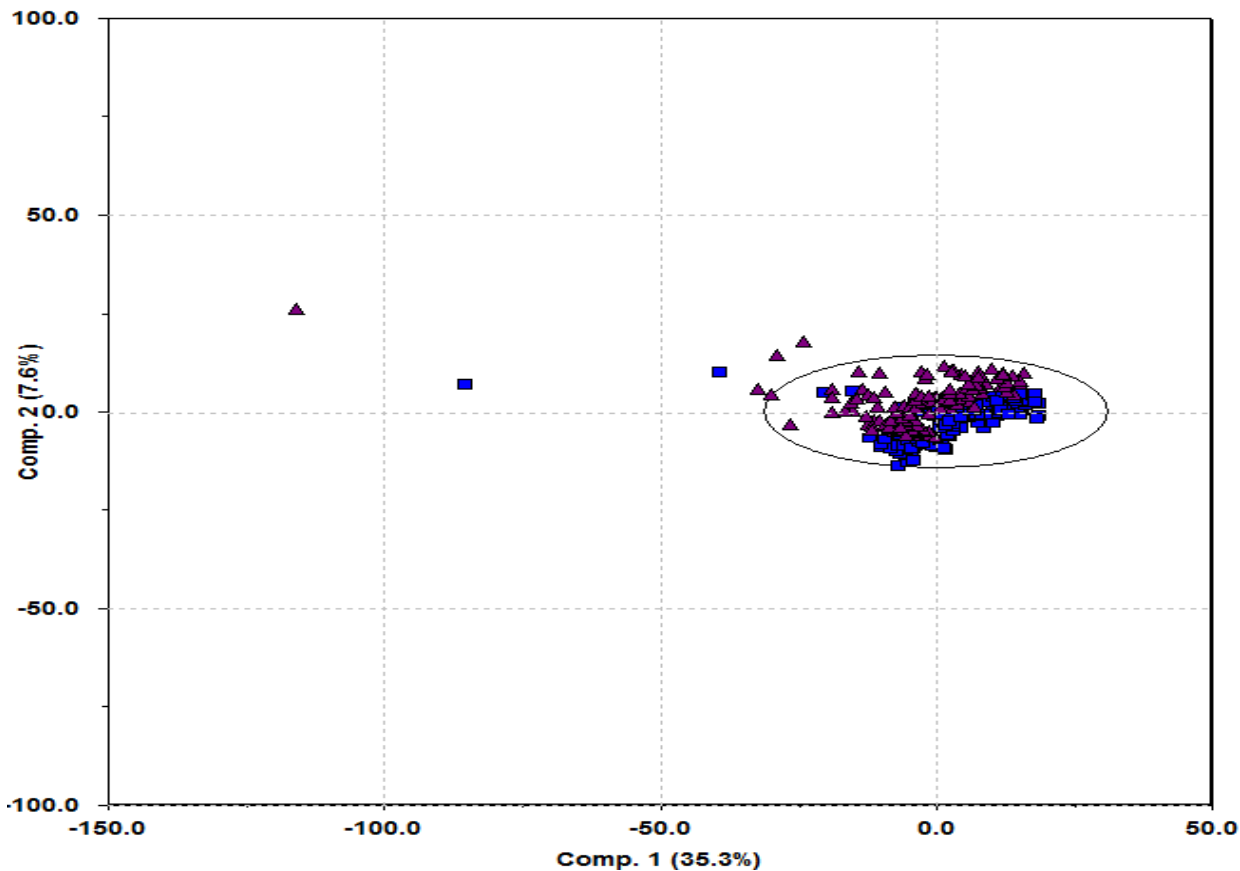


**Figure 4.19:** Score plot for first two similar runs, first (□) and second ( $\Delta$ ) for Reaction 2 in the reactor

### 4.3.3 Reaction 3

#### 4.3.3.1 Batch reaction

The raw Raman data set for Reaction 3 in batch is presented in Fig. 4.20. It is obvious that two regions ( $1050$  and  $550\text{ cm}^{-1}$ ) were visible. The band around  $1050\text{ cm}^{-1}$  was more prominent than for the batch runs of the previous reactions. This fact proposed that most of the substrate was substituted with Br and hence more product was obtained. This fact was verified by offline NMR analysis which showed that 98% of the substrate was converted to yield product (80%). The intensity pattern of two characteristic Raman frequencies ( $550$  and  $1050\text{ cm}^{-1}$ ) showed that Br substitution increased as the reaction proceeded and started decreasing near the end of the reaction whereas intensity for  $550\text{cm}^{-1}$  increased linearly throughout the reaction (Fig. 4.21).

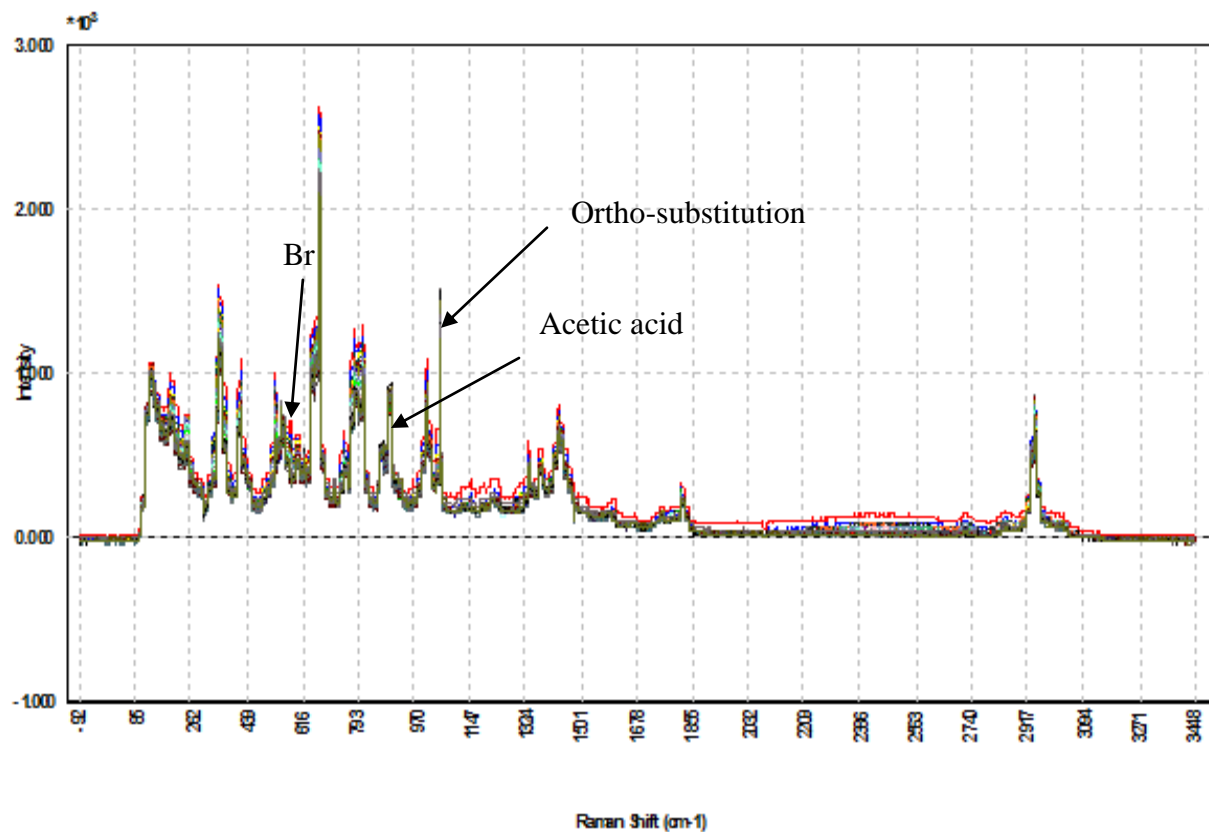


**Figure 4.20:** Raw Raman spectral data for Reaction 3 under batch conditions

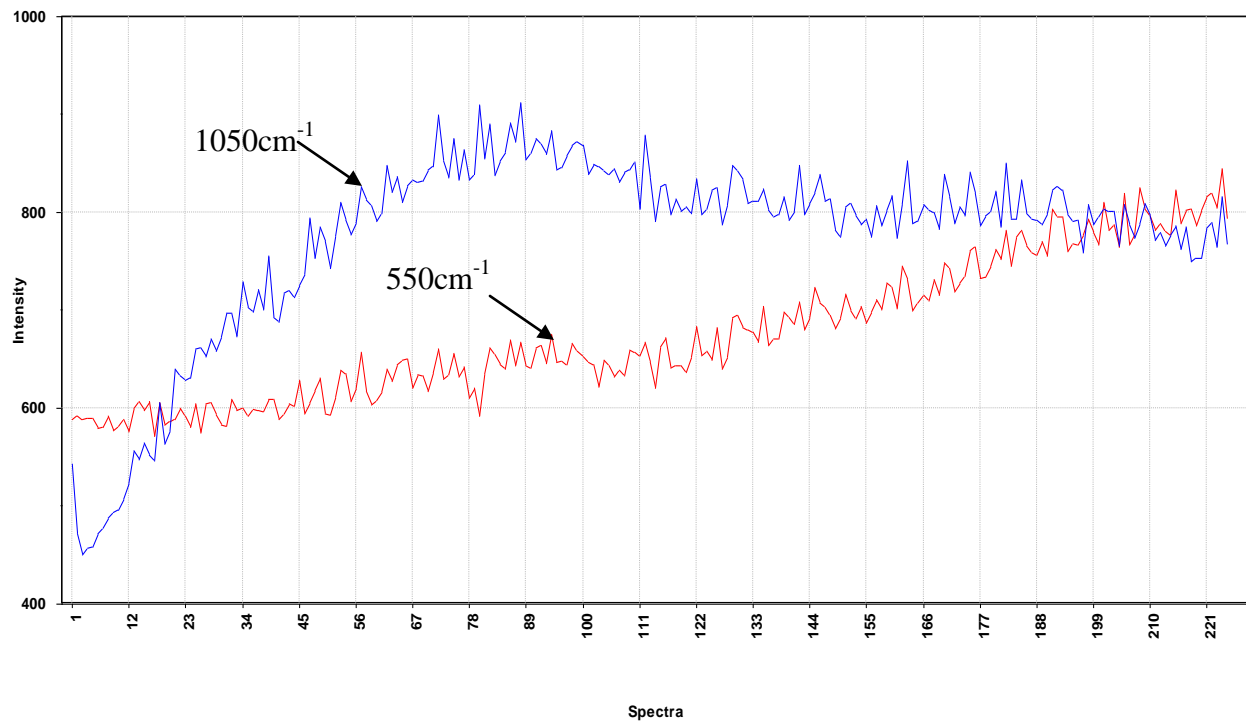


**Figure 4.21:** Intensity plot for Raman frequencies,  $1050\text{ cm}^{-1}$  and  $550\text{ cm}^{-1}$ , for Reaction 3 under the batch conditions

The respective two PCs score plot for this reaction also showed a similar evolutionary profile of the reaction (Fig. 4.22). Some of the spectra during the start of the reaction were found outside the Hotelling  $T^2$  ellipse implying the initial adjustment of the Raman system. The respective reaction profile based on score values for first two PCs is given in Fig. 4.23. The score trace for the first PC showed the progress of the reaction in terms of product formation whereas the second PC explained the behavior of reactants over time. The second PC implied the formation of the intermediate which was then consumed by the end of reaction. This phase lasted from 8 to 24 minutes. It was also note worthy that the intensity plot for Raman frequency ( $894\text{ cm}^{-1}$ ) also shared similar findings (Appendix 1, Fig. A9).

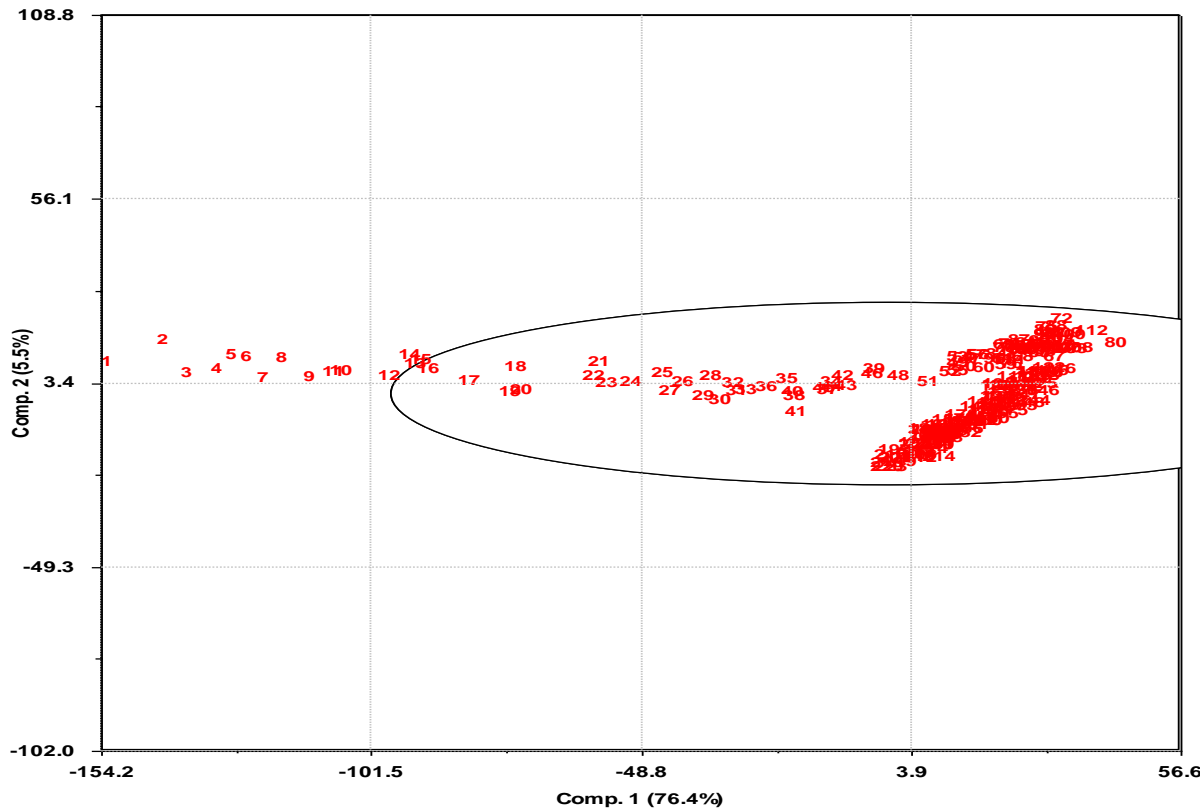


**Figure 4.22:** Score plot for Reaction 3 under the batch conditions

The distribution of the score values of the spectra could be explained on the basis of biplot (Appendix 1, Fig. A10). This plot differentiated the start and end of reaction on the basis of Raman frequencies around  $550$  and  $1050\text{ cm}^{-1}$ . These frequencies were responsible for the formation of the product. The loop of frequencies around  $650$ - $680\text{cm}^{-1}$  showed the presence of acetic anhydride in the reaction mixture. However, a peak close to  $894\text{ cm}^{-1}$  after the start of the reaction was observed which could be due to the hydrolysis of acetic anhydride to acetic acid in the reaction mixture<sup>55</sup>. This fact was further explained by the intensity plot (Appendix 1, Fig. A9) which revealed that Raman intensity at  $894\text{ cm}^{-1}$  decreased during the first eight minutes and

then it started increasing for the next eight minutes and remained constant thereafter. It could be argued that the solvent in the reaction mixture experienced some chemical change which was then disappeared. The respective loading plot was given in Appendix 1, Fig. A11.

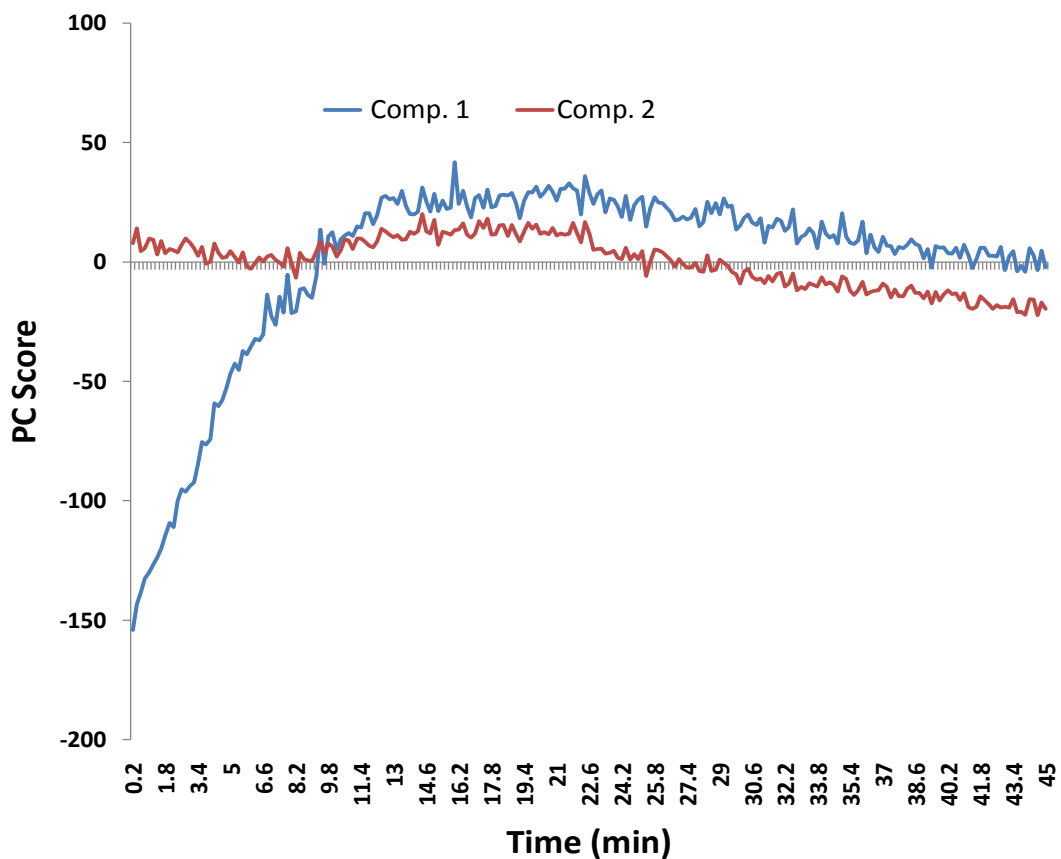


**Figure 4.23:** Reaction profile based on score values of the first two PCs for Reaction 3 under batch conditions

#### 4.3.3.2 MJOD reaction

The combined raw Raman data set for two runs of Reaction 3 in the reactor is presented in Fig. 4.24. The behavior of the spectra was found to be similar to the batch reaction. The Raman band at  $1050\text{cm}^{-1}$  was more prominent than for the previous reactions in the reactor. Similarly, the band at  $894\text{ cm}^{-1}$  was also found to be much intense than in the previous reactions.

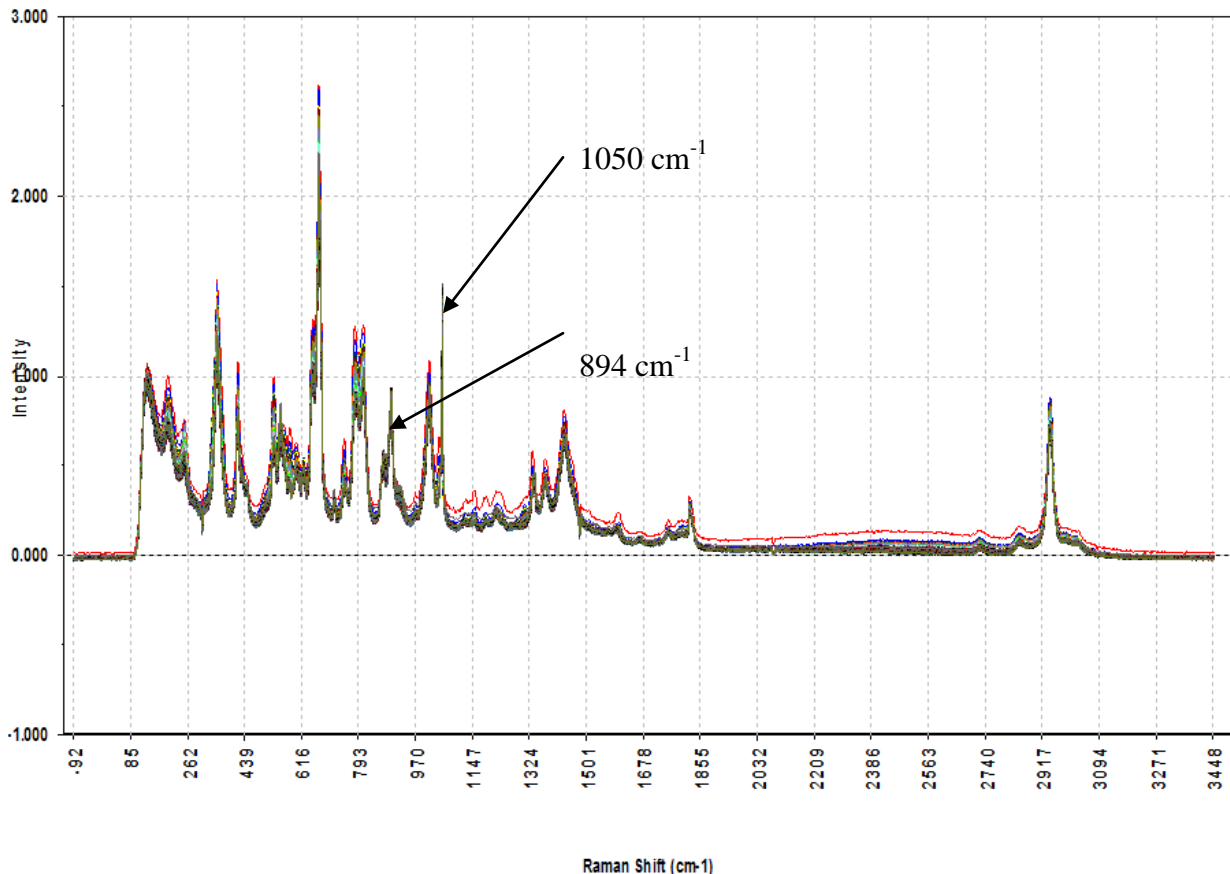


**Figure 4.24:** The combined raw Raman data set for two runs of Reaction 3 in the reactor

The score plot based on the first two PCs (Fig. 4.25) depicted the abnormal intensity in some of the Raman bands like  $1050\text{cm}^{-1}$ . It showed that second run ( $\Delta$ ) in the reactor was different from the first run ( $\square$ ). The first run was grouped as one group than the second run where some kind of sub-grouping could be seen. Even some of the spectra from the second run were moving away from the sub-grouping. This fact showed that second run observed some drastic change in its spectra after certain period of time.

The respective biplot (Fig. 4.26) revealed that two runs could be distinguished on the basis of Raman bands around  $1040\text{-}1055\text{ cm}^{-1}$ . These bands were found characteristic for ortho substitution in the substrate to form the product. Thus, Raman spectra of two runs in the reactor were plotted separately to investigate respective peak positions (Fig 4.27-28).

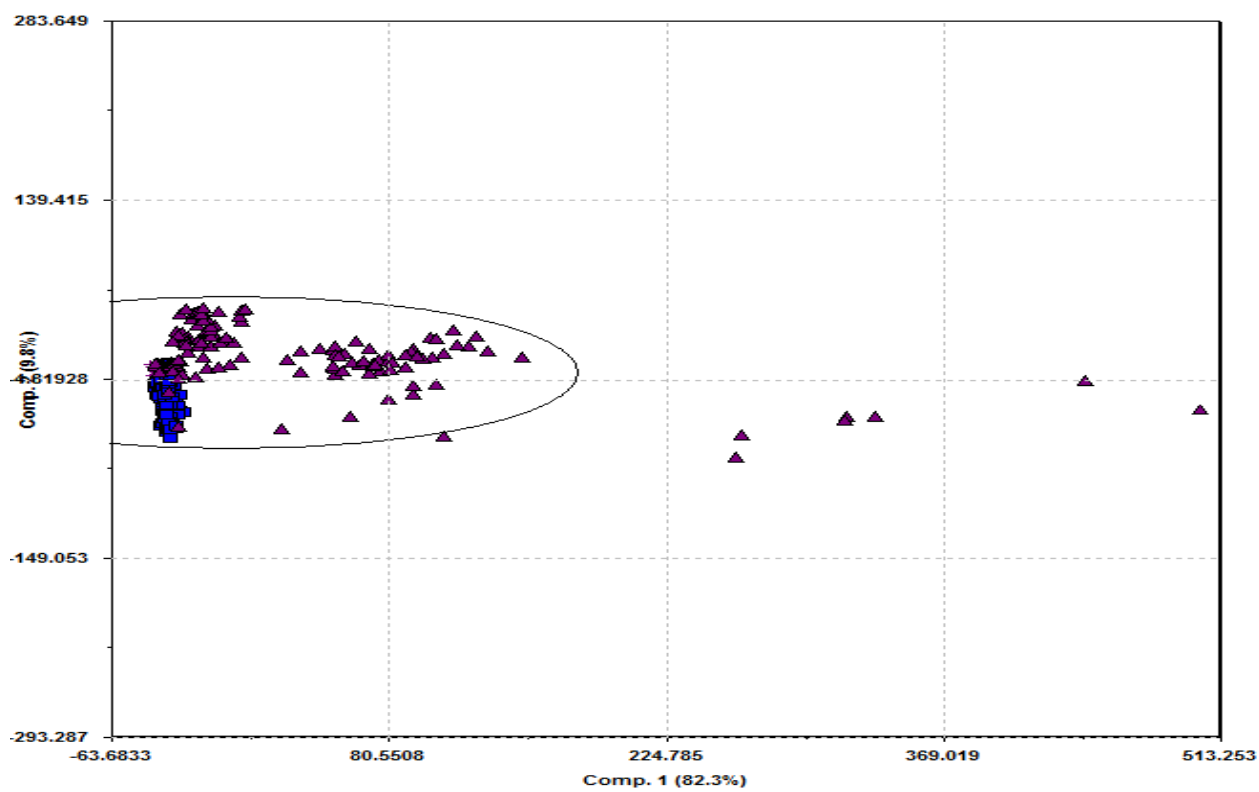


**Figure 4.25:** Score plot of two runs in the reactor for Reaction 3; the first run (□) and the second run ( $\Delta$ )

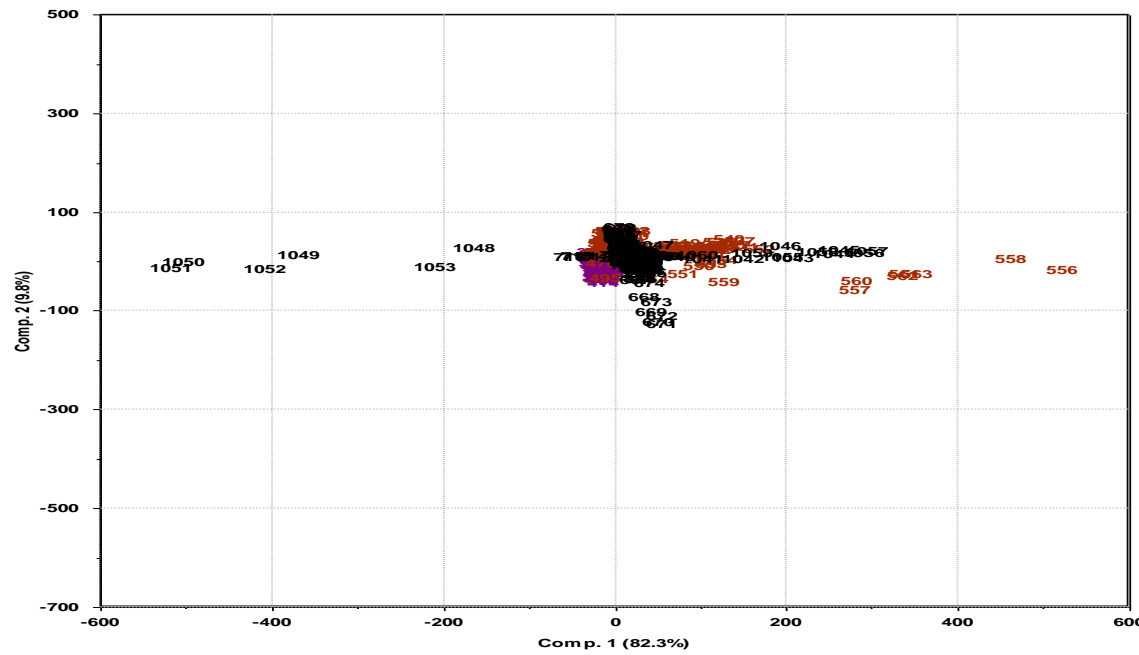


**Figure 4.26:** Bilpot of two runs in the reactor for Reaction 3

It was noticed that in case of the first run, only peak at  $894\text{ cm}^{-1}$  was found prominent than the previous experiments. The intensity plot for this frequency showed that intensity at  $894\text{ cm}^{-1}$  linearly decreased during the run (Appendix 1, Fig. A12). The signal for acetic acid could be found due to the presence of water inside the reactor which was used for washing in order to remove unreacted KBr after the reaction. This water could hydrolyze acetic anhydride to acetic acid at the start of the run and could be carried over by the solvent later on. That could be the reason for linear decrease in the intensity at  $894\text{ cm}^{-1}$  as a function of time. The first run yielded 69% of the product with 100% conversion of the substrate.

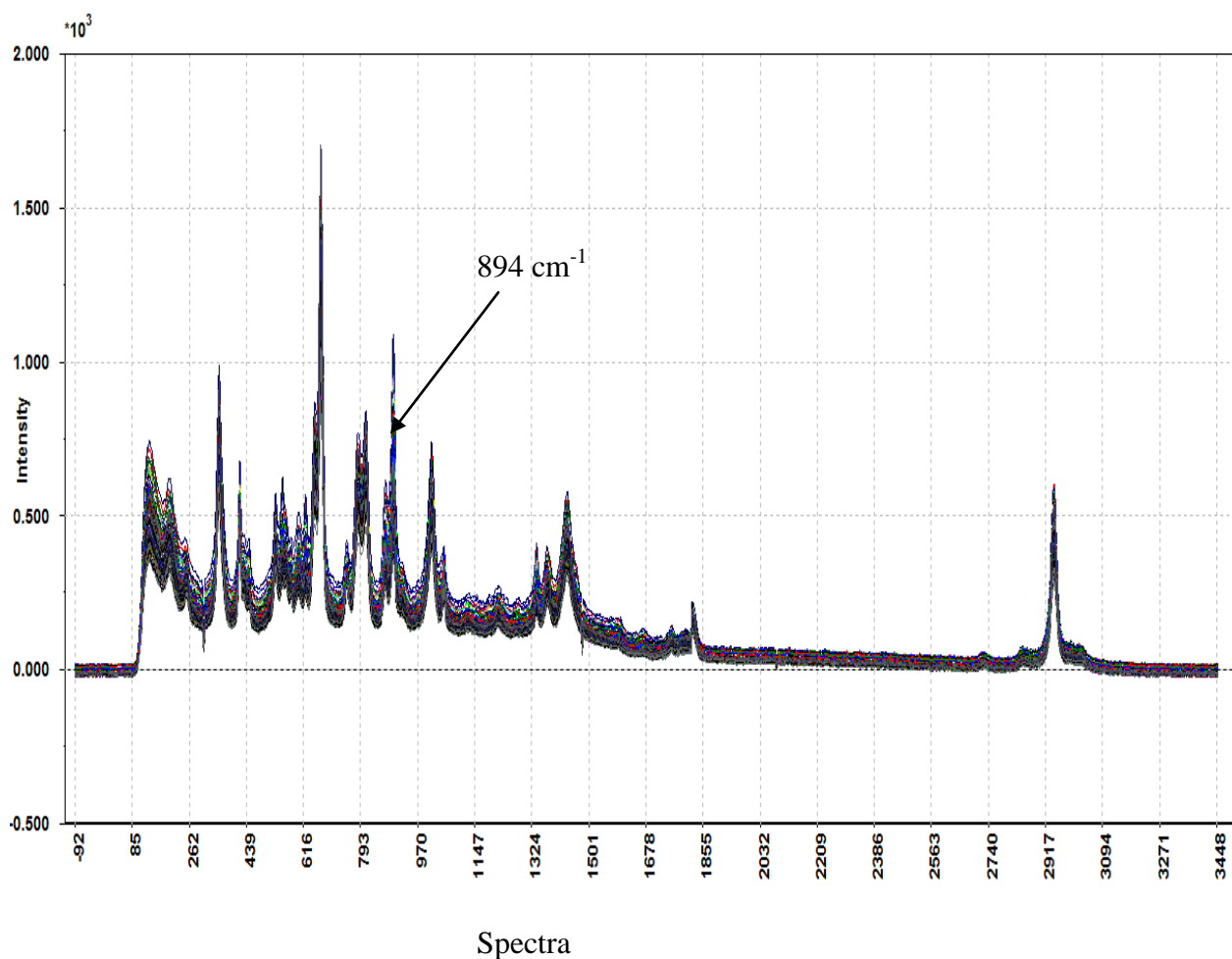


**Figure 4.27:** Raw Raman data for the first run in the reactor for Reaction 3

The inspection of raw Raman data set plot for the second run in the reactor revealed that Raman band characteristic for ortho substitution ( $1050\text{ cm}^{-1}$ ) was more intense than for the previous

experiments (Fig. 4.28). The behavior of this band was quite similar to the reaction carried out under the batch conditions.

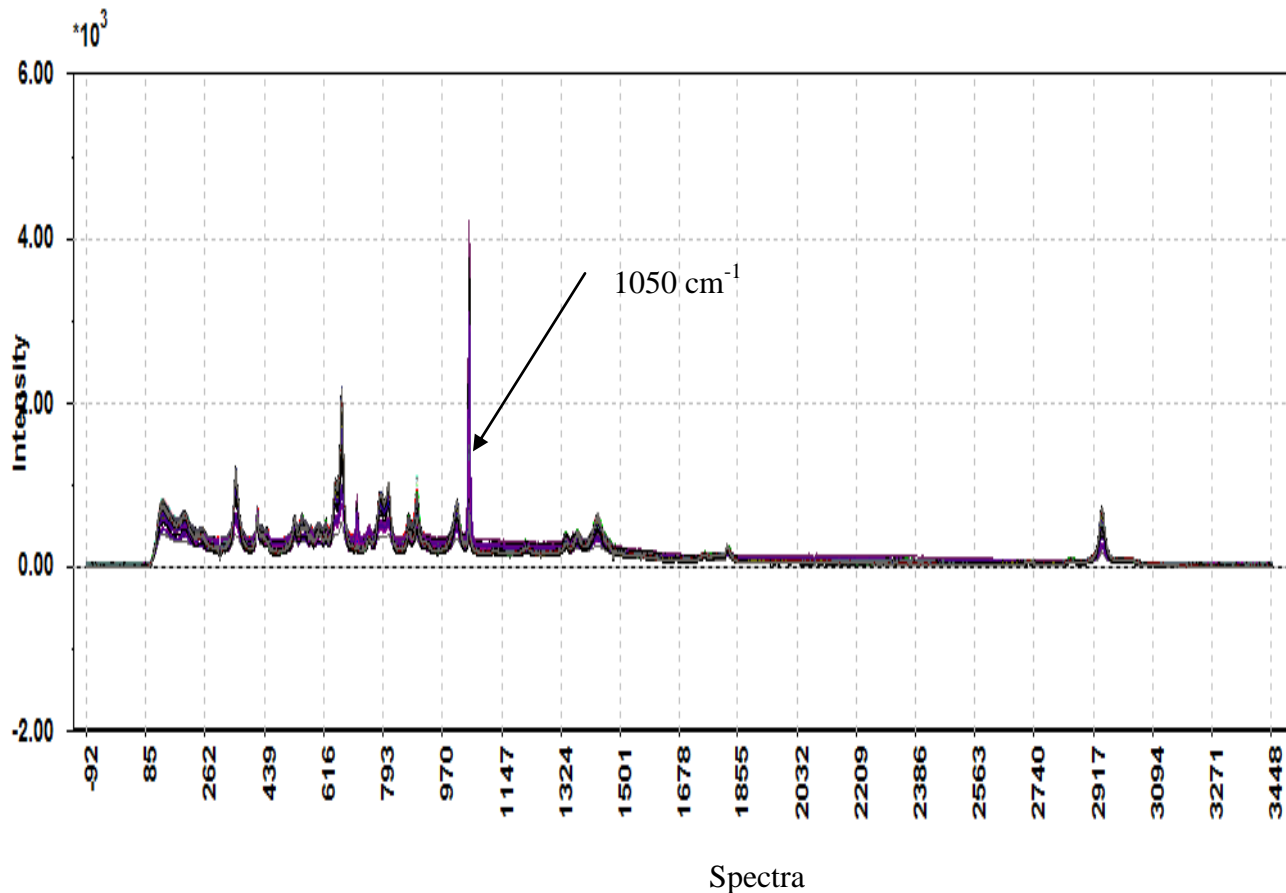


**Figure 4.28:** Raw Raman data for the second run in reactor for Reaction 3

The intensity plot for 550 and 1050 cm<sup>-1</sup> showed that the intensity at 1050 cm<sup>-1</sup> suddenly oscillated for only two minutes during the monitoring (Fig. 4.29). Meanwhile, no increase could be observed at 550 cm<sup>-1</sup>. It could be argued that it could happen due to the presence of unreacted substrate in the stream for a limited time. Another reason for this behavior could be due to the formation of a byproduct (2,6-dibromo-3,4,5-trimethoxytoluen) which was observed during some other lab studies. The offline result supported this argument because a 98% conversion of the substrate could yield only 63% of the product.

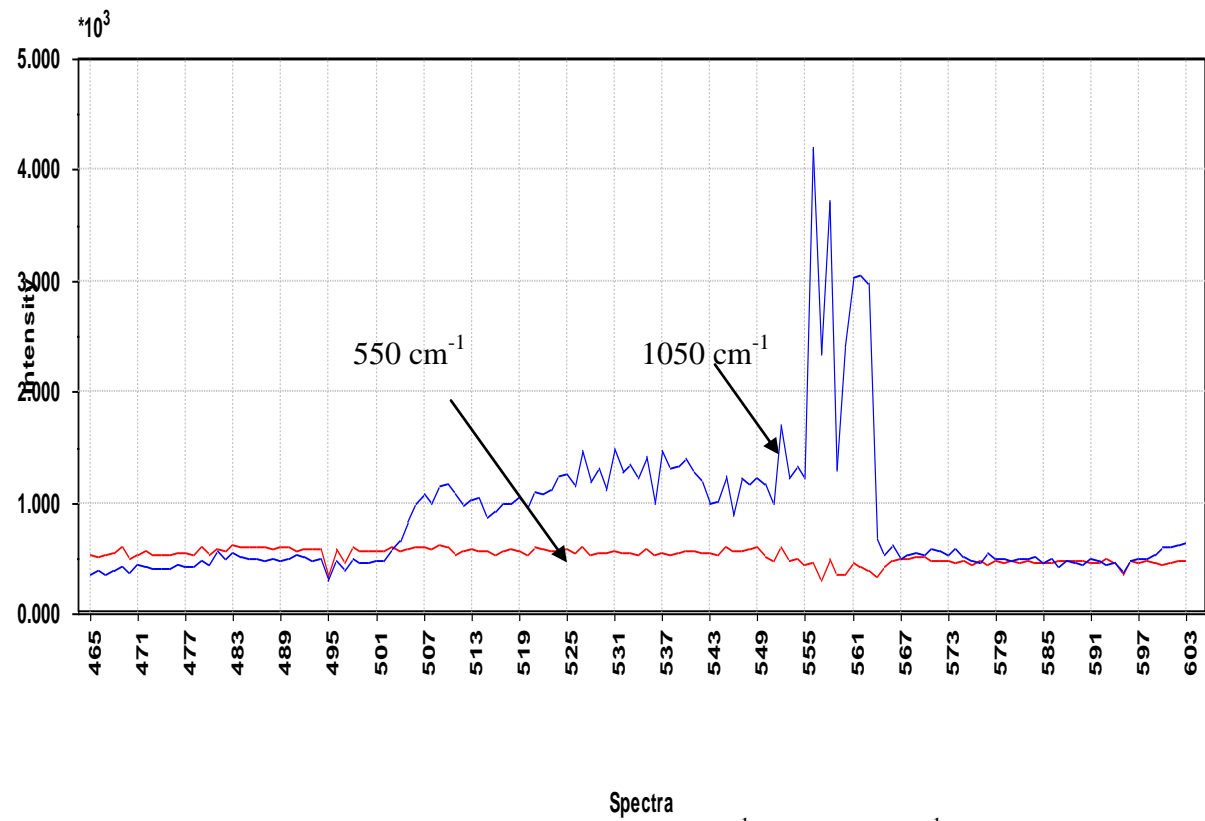


**Figure 4.29:** The intensity plot for Raman bands at  $550\text{ cm}^{-1}$  and  $1050\text{ cm}^{-1}$  for the second run in the reactor for Reaction 3

## **5. Conclusions and Future Perspective**

An inline analytical method based on the optical fiber Raman spectroscopy has been successfully demonstrated for the monitoring of organic syntheses under the batch as well as continuous flow conditions. The laser-induced Raman spectroscopy has been proved a powerful tool for the real time monitoring of the organic reactions. Raman spectroscopy does not interrupt the process whereas its signal can detect any malfunctioning of the process immediately. This technique has been successful for monitoring the synthesis of 2-bromo-3,4,5-trimethoxytoluene under the different set of conditions, however it could be explored for several organic reactions. It is attributed to the highly sensitive measurements and easy to handle for the both type of assignments (batch and continuous processes). The Raman spectroscopy also presents the information about the chemical and structural properties of a sample.

In the present study, the synthesis of 2-bromo-3,4,5-trimethoxytoluene has been investigated under the batch and continuous conditions employing an optical fiber Raman spectroscopy as an inline analytical technique. The NMR has been used as an offline analytical technique to verify the results obtained by the Raman spectroscopy. Raman spectroscopy has experienced no effect on its measurements from the potential process disturbances; the oscillator and the feeding pumps. Three different synthesis reactions with three different concentrations of the substrate were used for this investigation. All the variations occurred during the process were successfully monitored and properly reported by the measurement system employing the two components PCA. These variations include, the temperature effect, pump breakage, back mixing in the reactor, lower conversion of the substrate and lower yield of the product etc. The results obtained by the spectroscopy have been verified by the NMR. Thus, the optical fiber Raman spectroscopy using an appropriate chemometric tool can be used as a reliable, sensitive and rapid process monitoring technique under the batch and continuous flow conditions.

As a part of the suggestions for future investigation, the spectroscopic measurements should be recorded for an organic reaction in the reactor over a longer period of time ( $>24\text{h}$ ). This investigation will reveal the information about the stability of both the constituents of the system; the reactor and the measurement system. Secondly, a calibration model should be employed for the direct estimation of the product from the reactor in order to get a quick inference about the yield of the product. Thirdly, a moving score plot fitted with the Hotelling's  $T^2$  should be used in order to investigate the normal functioning of the process and to identify and locate the potential disturbances (if exist) continuously.

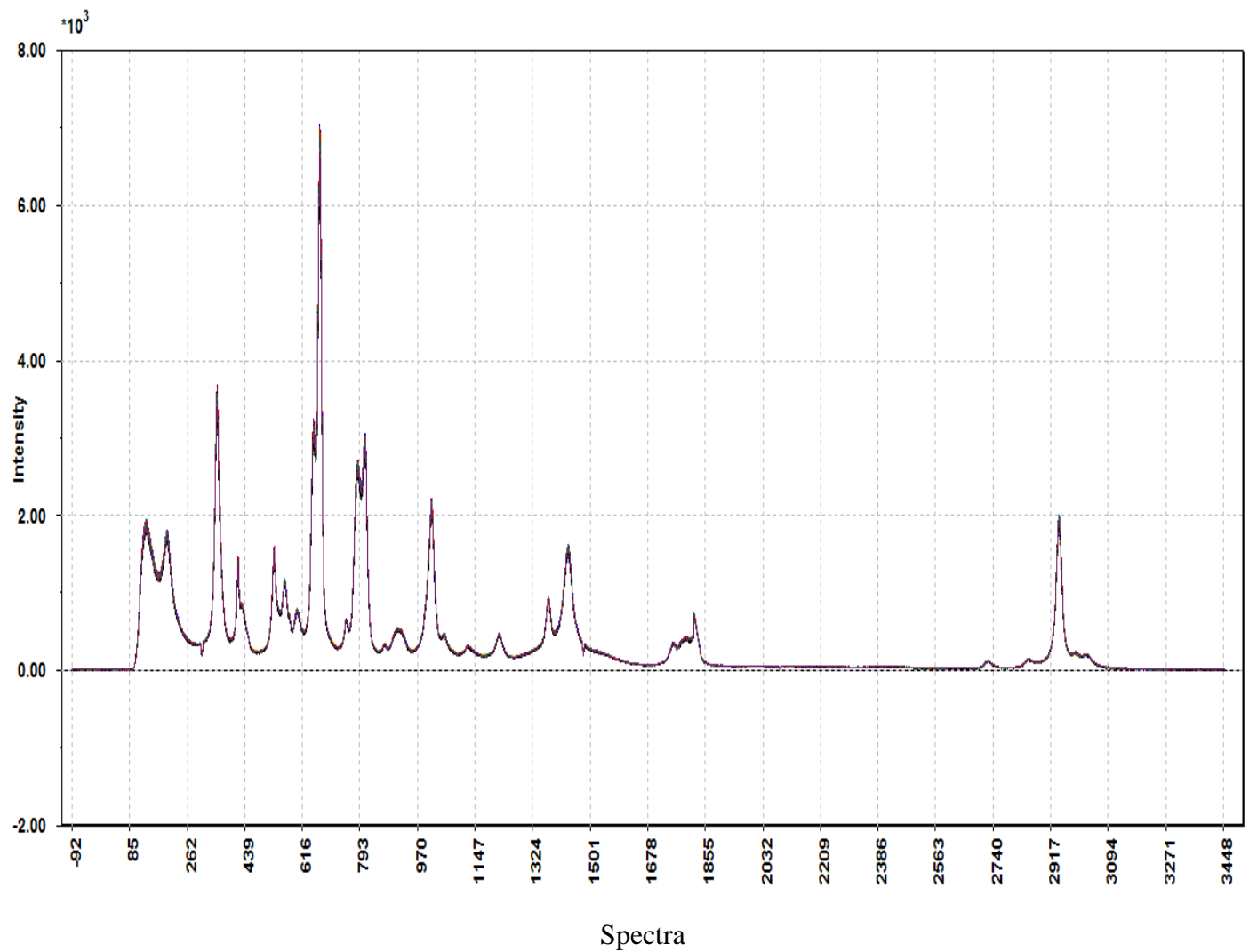
## Reference

1. Cervera, A.E.; Skovby, T.; Kiil, S.; GAni, R.; Gerneay, K. *Moving from batch towards continuous organic chemical pharmaceutical production.* AIChE Annual Meeting, 8-13 Novemeber, Nashville, USA, 2009.
2. Kee, S.P.; Gavriliidis, A. *J. Mol. Catal A: Chem.* **2007**, 263, 156.
3. Fletcher, P. D. I.; Haswell, S. J.; Pombo-Viller, E.; Warrington, B. H.; Watts, P.; Wong, S. Y. F.; Zhang, X. *Tetrahedron.* **2002**, 58, 4735.
4. [http://courses.washington.edu/microflo/Group\\_A/whatmr1.htm](http://courses.washington.edu/microflo/Group_A/whatmr1.htm)
5. [http://www.fluensynthesis.com/How\\_MJOD\\_works.html](http://www.fluensynthesis.com/How_MJOD_works.html)
6. US Food and Drug Administration. *Guidance for industry PAT-A framework for innovative Pharmaceutical development, manufacturing and quality assurance,* USA, 2004.
7. Ferstl, W.; Klahn, T.; Schweikert, W.; Billeb, G.; Schwarzer, M.; Loebbecke, G. *Chem. Eng. Technol.* **2007**, 30, 370.
8. Jacques, W.; Zilian, A. *Org. Proc. Res. Dev.* **2003**, 7, 1059.
9. Reis, M. M.; Uliana, M.; Sayer, C.; Araújo, P. H. H.; Giudici, R. *Braz. J. Chem. Eng.* **2005**, 22, 61.
10. Svensson, O.; Josefson, M.; Langkilde, F. W. *Eur. J. Pharm. Sci.* **2000**, 11, 141.
11. Kourtzi, T. *Anal. Bioanal. Chem.* **2006**, 384, 1043.
12. <http://www.fda.gov/cder/OPS/PAT.htm>
13. US Food and Drug Administration. *PAT: A Framework for Innovative Manufacturing and Quality Assurance, Guidance for Industry.* US Food and Drug Administration, Washington, 2003.
14. Bruneel, J. L.; Lassegues, J. C.; Sourisseau, C. *J. Raman. Spectrosc.* **2002**, 33, 815.
15. Jeon, S.; Woo, J.; Kyong, J. B.; Choo, J. *Bull. Korean. Chem. Soc.* **2001**, 22, 1264.
16. Jeon, S.; Choo, J.; Kim, S.; Kwon, Y.; Kim, J.; Lee, Y.; Chung, H. *J. Mol. Struct.* **2002**, 609, 159.
17. Smith, E; Dent, G. *Modren Raman Spectroscopy-A Practical Approach.* Wiley, West Sussex, 2005.
18. : [www.scielo.org.ar/scielo.php?pid=S0365-037520](http://www.scielo.org.ar/scielo.php?pid=S0365-037520)
19. Vankeirsbilck, T; Vercauteren, A.; Baeyens, W.; Van der Weken, G. *Trends. Ana. Chem.* **2002**, 21, 869.
20. McCreery, R.L. *Raman Spectroscopy for Chemical Analysis,* Wiley, West Sussex, 2000.
21. Lee, M; Kim, H; Rhee, H; Choo, J. *Bull. Korean Chem. Soc.* **2003**, 24, 205.
22. [http://www.ibscaribe.com/news/Practical\\_Considerations.htm](http://www.ibscaribe.com/news/Practical_Considerations.htm)
23. Cogdill, R. P.; Anderson, C. A; Delgado, M.; Chisholm, R.; Bolton, R.; Herkert, T.; Afnan, A. M.; Drennen, J. K. *AAPS. Pharm. Sci. Technol.* **2005**, 6, E273
24. Blanco, M.; Villarroya, I. *Trends. Ana. Chem.* **2002**, 21, 240.

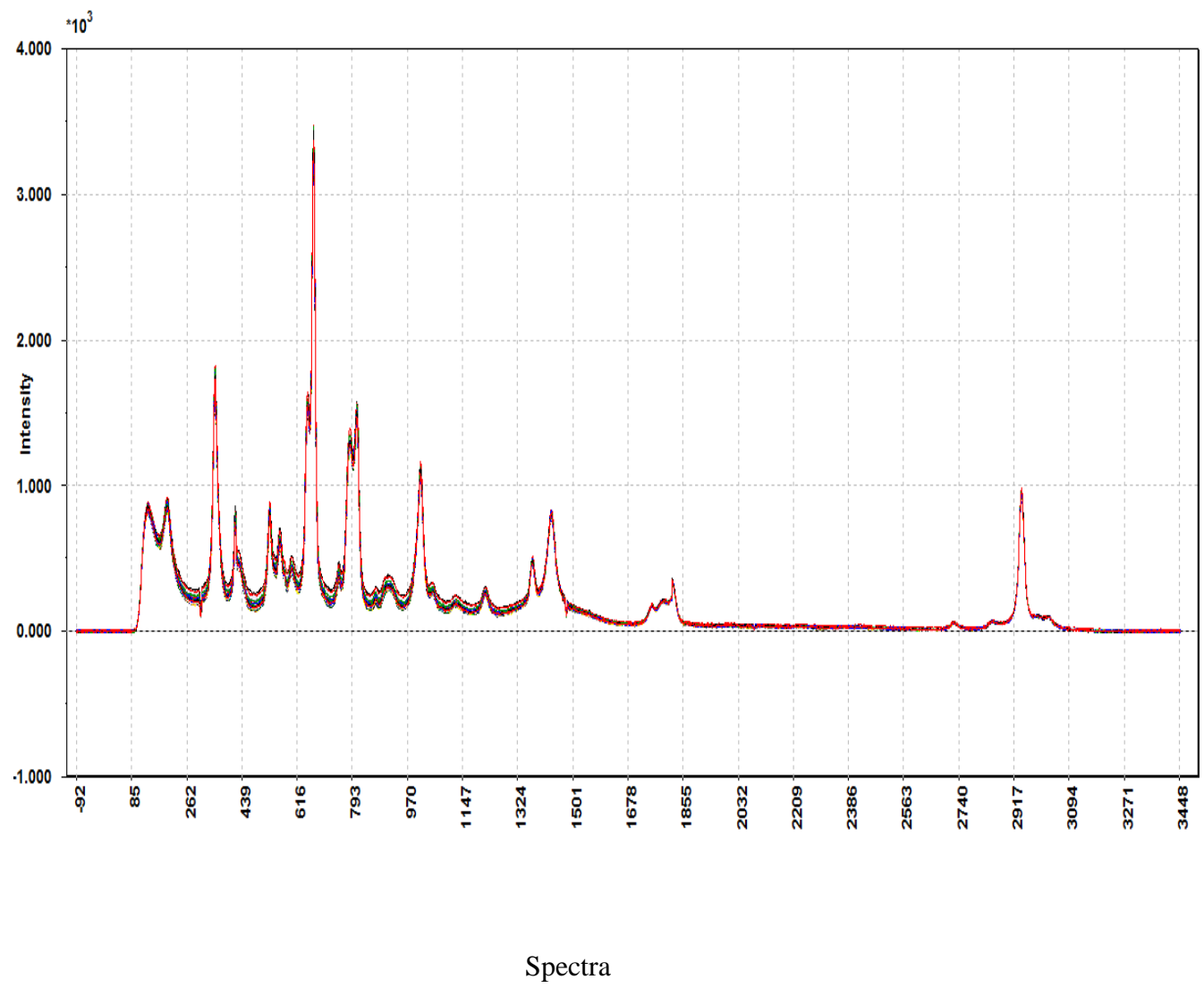
25. Zeaiter, M.; Roger, J. M.; Bellon-Maurel, V.; Rutledge, D. N. *Trends Anal Chem.* **2004**, 23, 157.
26. Griffiths, P.J. *J. Near. Infrared. Spectrosc.* **1995**, 3, 60.
27. Workman, J. J. Jr.; Mobley, P. R.; Kowalski, B. R.; Bro, R. *Appl. Spectrosc. Rev.* **1996**, 31, 73.
28. Mobley, P. R.; Kowalski B. R.; Workman, J. J. Jr.; Bro, R. *Appl. Spectrosc. Rev.* **1996**, 31, 347.
29. Breton. R. G. *Chemometric-Data Analysis for the Laboratory and Chemical Plant*. Wiley, West Sussex, 2003.
30. Geladi, P.; McDougall, D.; Martens, H. *Appl. Spectrosc.* **1985**, 39, 491.
31. Barnes, R.J.; Dhanoa, M.S.; Lister, S. J. *Appl. Spectrosc.* **1989**, 43, 772.
32. Brown, S. D.; Tauler, R.; Walczak, B. *Comprehensive Chemometrics: Chemical and Biochemical Data Analysis*. Elsevier, Amsterdam, 2009.
33. Laasonen, M.; Harmia-Pulkkinen, T.; Simard, C.; Rasanen, M.; Vuorela, H. *Anal. Chem.* **2003**, 75, 754.
34. Widjaja, E.; Tan, Y. Y.; Garland, M. *Org. Proces. Res. Dev.* **2007**, 11, 98.
35. Blanco, M.; Serrano, D. *Analyst*, **2000**, 125, 2059.
36. Box, G. E. P.; Jenkins, G. M; Reinsel, G. C. *Time Series Analysis*. Prentice Hall, Upper Saddle River, 1994.
37. Jackson, J. E.; Mudholkar, G. S. *Technometrics*. **1979**, 21, 341.
38. Martens, H.; Naes, T. *Multivariate Calibration*. Wiley, New York, 1989.
39. Naes, T.; Martens, H. *J Chemometr.* **1988**, 2, 155.
40. Wold, S.; Ruhe, A.; Wold, H.; Dunn, W. J. III. *SIAM J Sci Stat Comput.* **1984**, 5, 735.
41. Wold, S.; Esbensen, K.; Geladi, P. *Chemom. Int. Lab. Syst.* **1987**, 2, 37.
42. Svensson, O.; Josefson, M.; Langkilde, F.W. *Chemom. Intell. Lab. Syst.* **1999**, 49, 49.
43. Martin, E. B.; Morris, A. J.; Papazoglou, M. C.; Kiparissides, C. *Comput. Chem. Engg.* **1996**, 20, S599 .
44. Wold, S. *Chemom. Intell. Lab. Syst.* **1994**, 23, 149.
45. Nijhuis, A.; Jong, S. D.; Vandeginste, B.G.M. *Chemom. Intell. Lab. Syst.* **1997**, 38, 51.
46. Shimoyama, M.; Maeda, H.; Matsukawa, K.; Inoue, H.; Ninomiya, T. *Vib. Spectrosc.* **1997**, 14, 253.
47. Wikstrom, C.; Albano, C.; Eriksson, L.; Friden , H.; Johansson , E.; Nordahl, A.; Rannar, S.; Sandberg, M.; Kettaneh-Wold, N.; Wold, S. *Chemom. Intell. Lab. Syst.* **1998**, 42, 221.
48. Kourtis, T. *J. PAT*, **2004**, 1, 13.
49. Kourtis, T. *J. PAT*, **2004**, 3, 18.
50. Choi, S. W.; Martin, E. B.; Morris, A. J.; Lee, I. *Ind. Eng. Chem. Res.* **2006**, 45, 3108.
51. Tsoukala, A; Liguori, L; Occhipinti, G; Bjorsvik, H. *Tetrahedron Lett.* **2009**, 50, 831.

52. Bjørsvik, H.-R.; Bjørsvik, L. L. Continuous flow reactor. PCT Int. ApplWO 2007058544 A1 20070524 , AN 2007:564470, 2007.
53. Mirone, P.; Fortunato, B.; Canziani, P. *J. Mol. Struct.* **1970**, *5*, 283.
54. Lin-Vien, D; Colthup, N. B; Fateley, W. G; Grasselli, J. G. *The Handbook of Infrared and Raman Characteristic Frequencies of Organic Molecules*; Academic Press: San Diego, 1991.
55. Bertie, J. E.; Michaelian, K. H. *J. Chem. Phys.* **1982**, *77*, 5267.

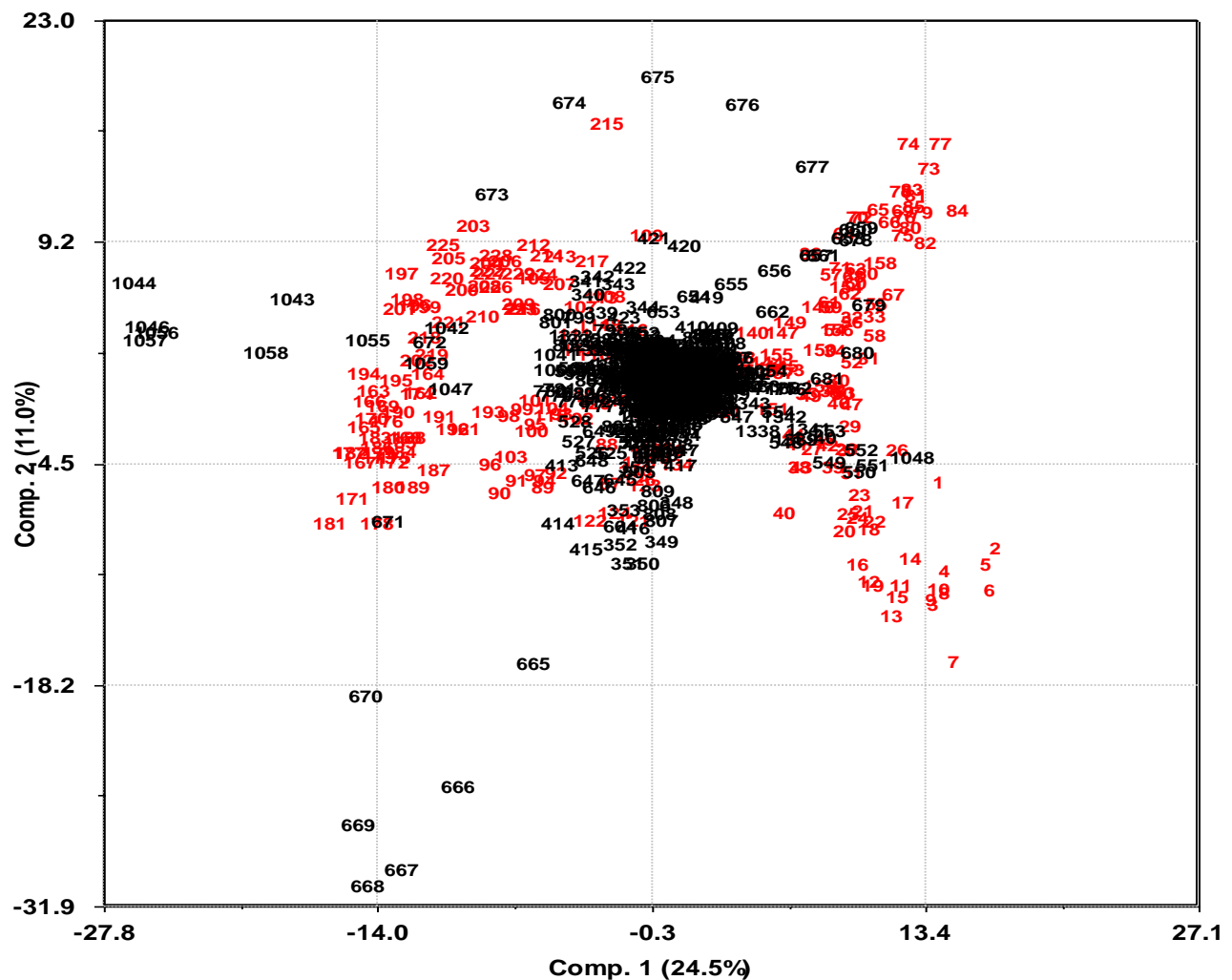
## Appendix 1



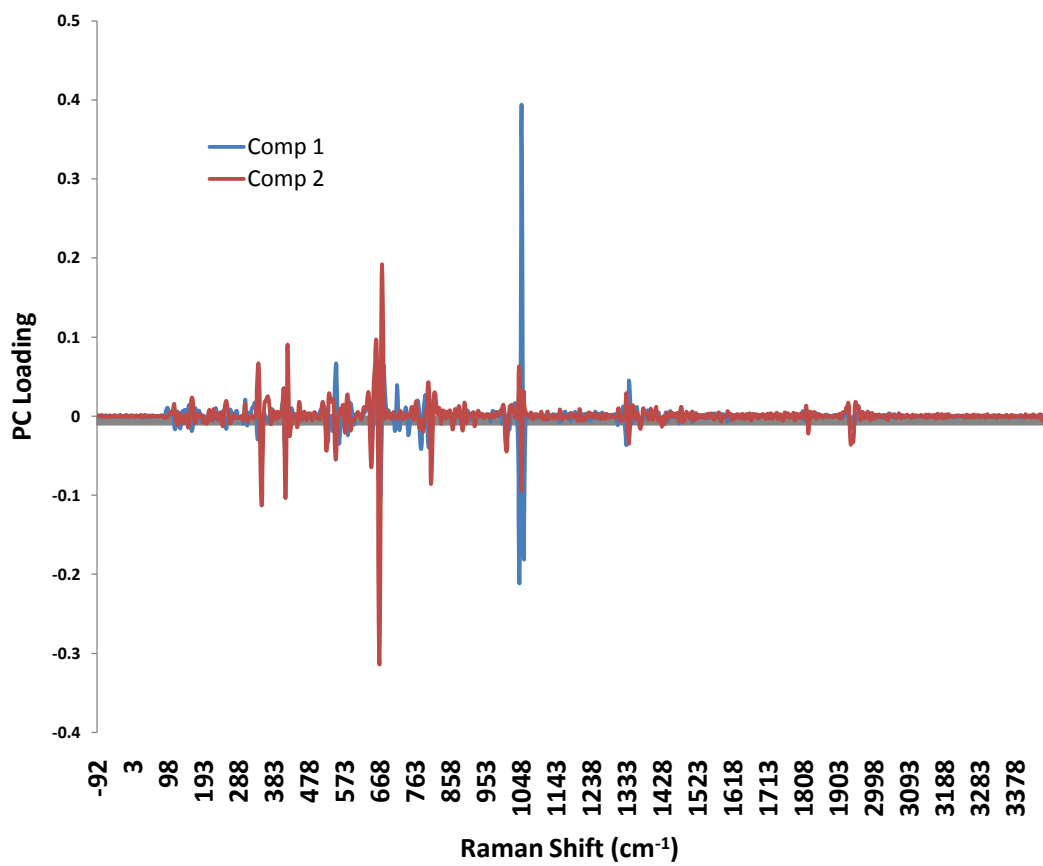
**Figure A.1:** Raw Raman spectra data for three different oscillator settings at a constant pump flow rate (2mL/min)



**Figure A.2:** Raw Raman data for various pump settings at constant oscillator setting (106 rpm)



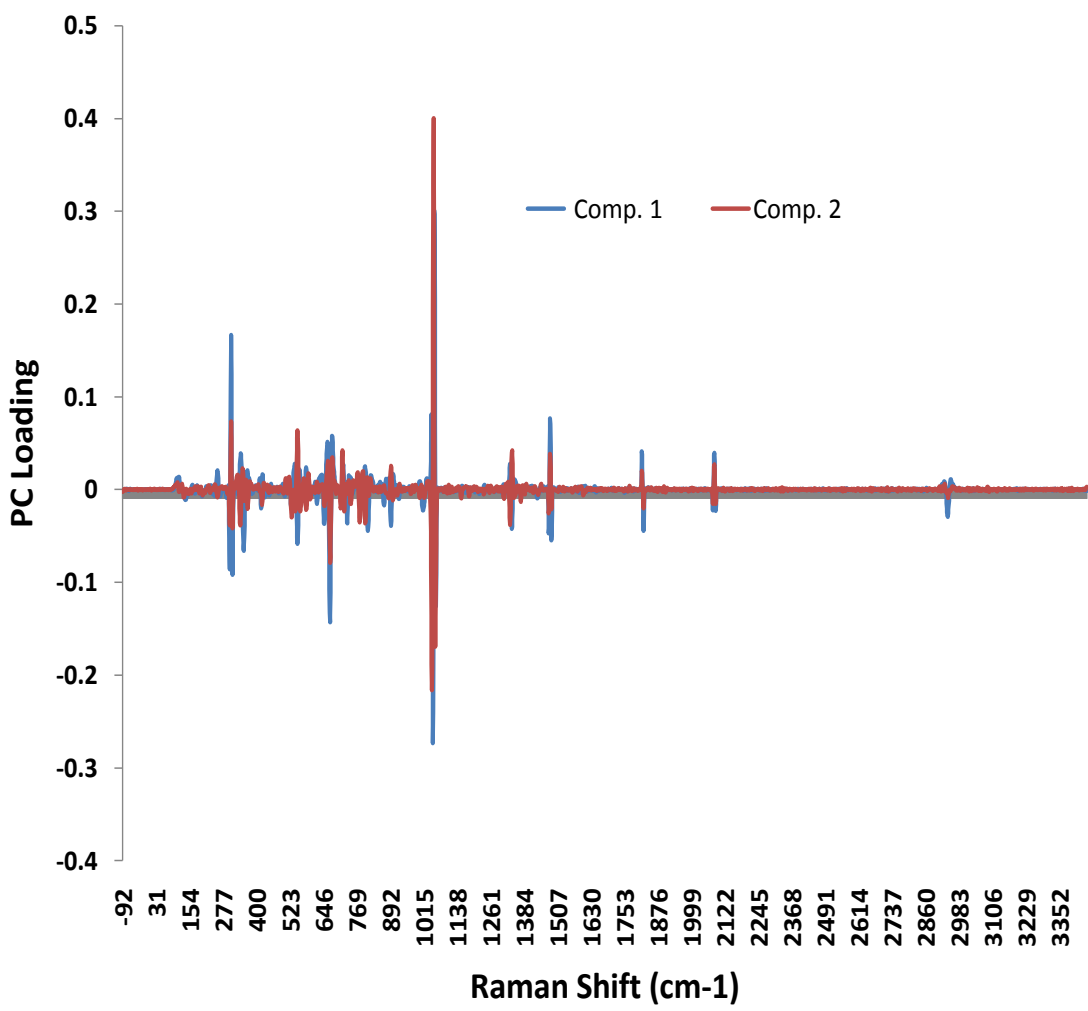
**Figure A 4.3:** Biplot for Reaction 1 under the batch conditions



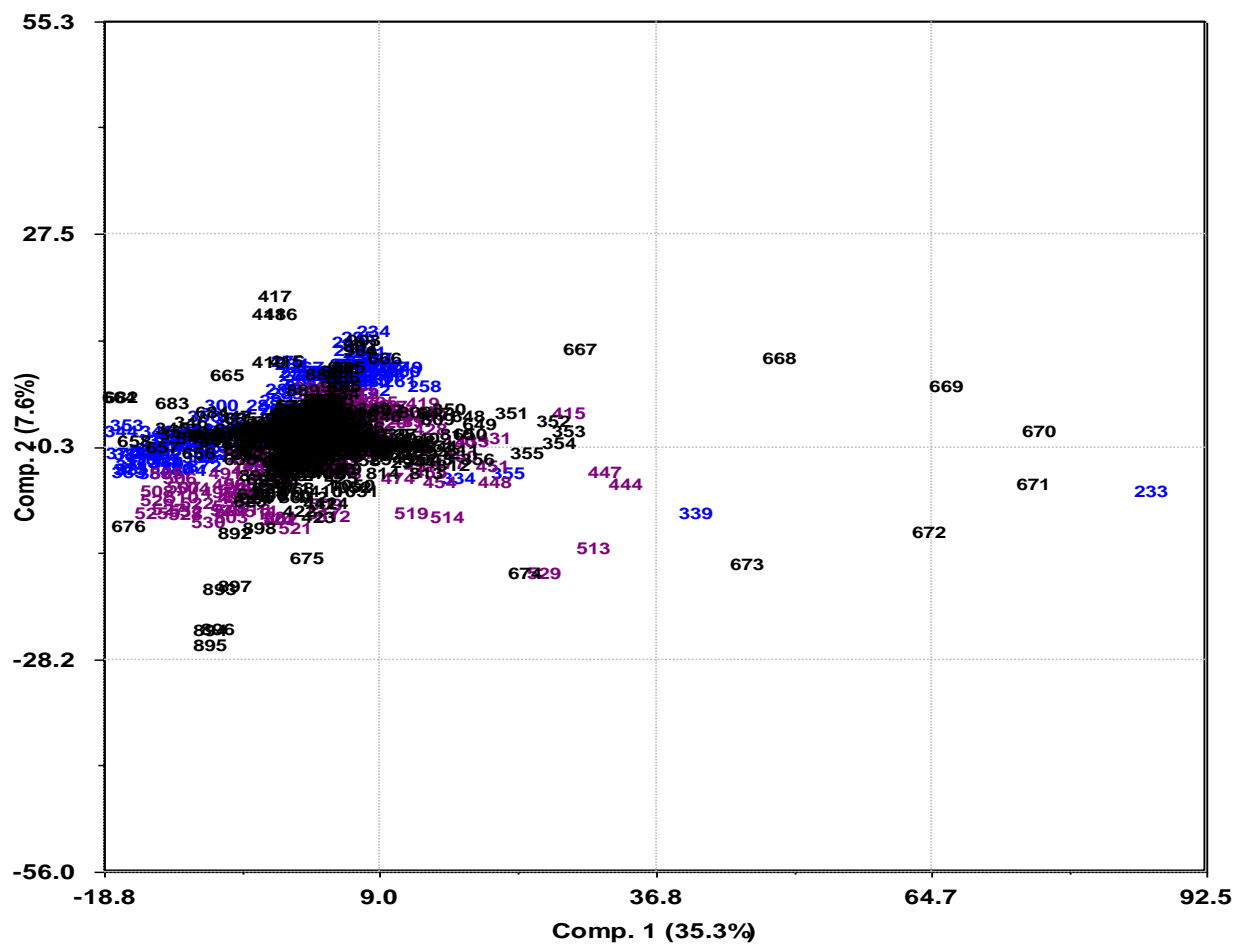
**Figure A.4:** Loading plot for Reaction 1 under the batch conditions

**Table A.5**Chemical data produced from offline analysis ( $^1\text{H}$  NMR)

<b>Reaction</b>	<b>Condition</b>	<b>Conversion (%)</b>	<b>Isolated Yield (%)</b>
1	Batch	89	59
	Reactor (R1)	85	49
	Reactor (R2)	86	60
2	Batch	97	79
	Reactor (R1)	95	58
	Reactor (R2)	98	64
	Reactor (R3)	72	34
3	Batch	98	80
	Reactor (R1)	100	69
	Reactor (R2)	98	63



**Figure A6:** Loading plot for Reaction 2 under the batch conditions



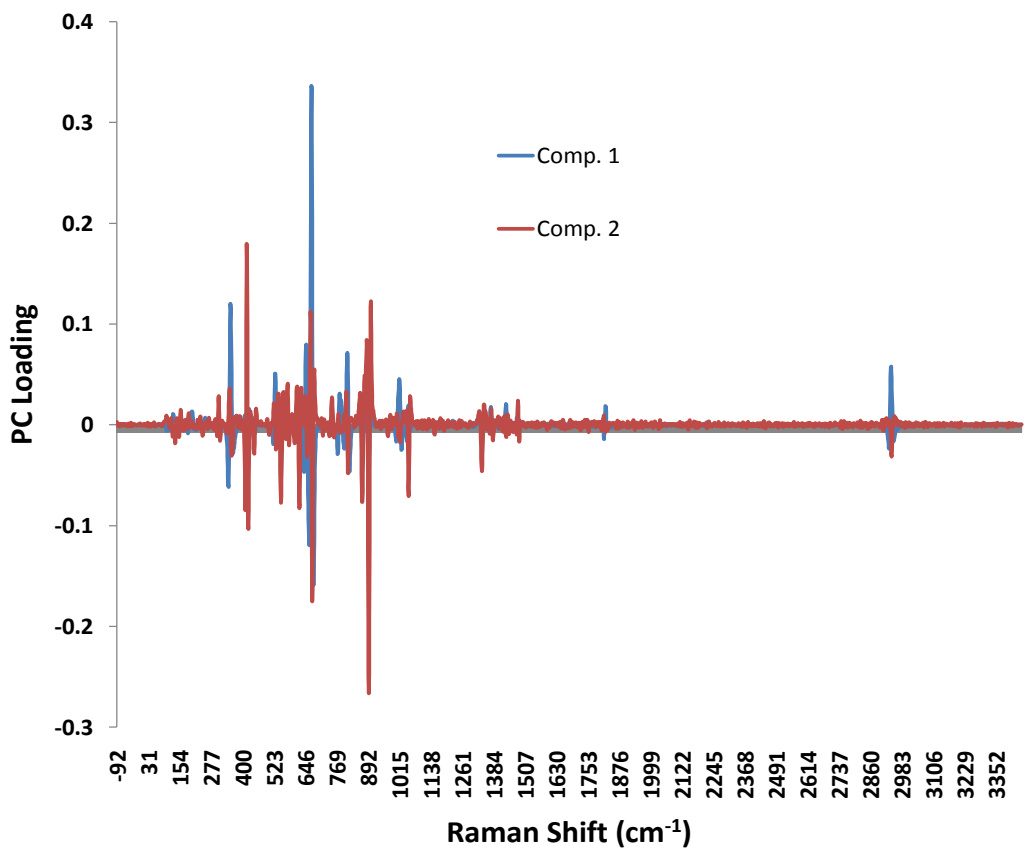


**Figure A8:** Loading plot of two similar runs for Reaction 2 in the reactor

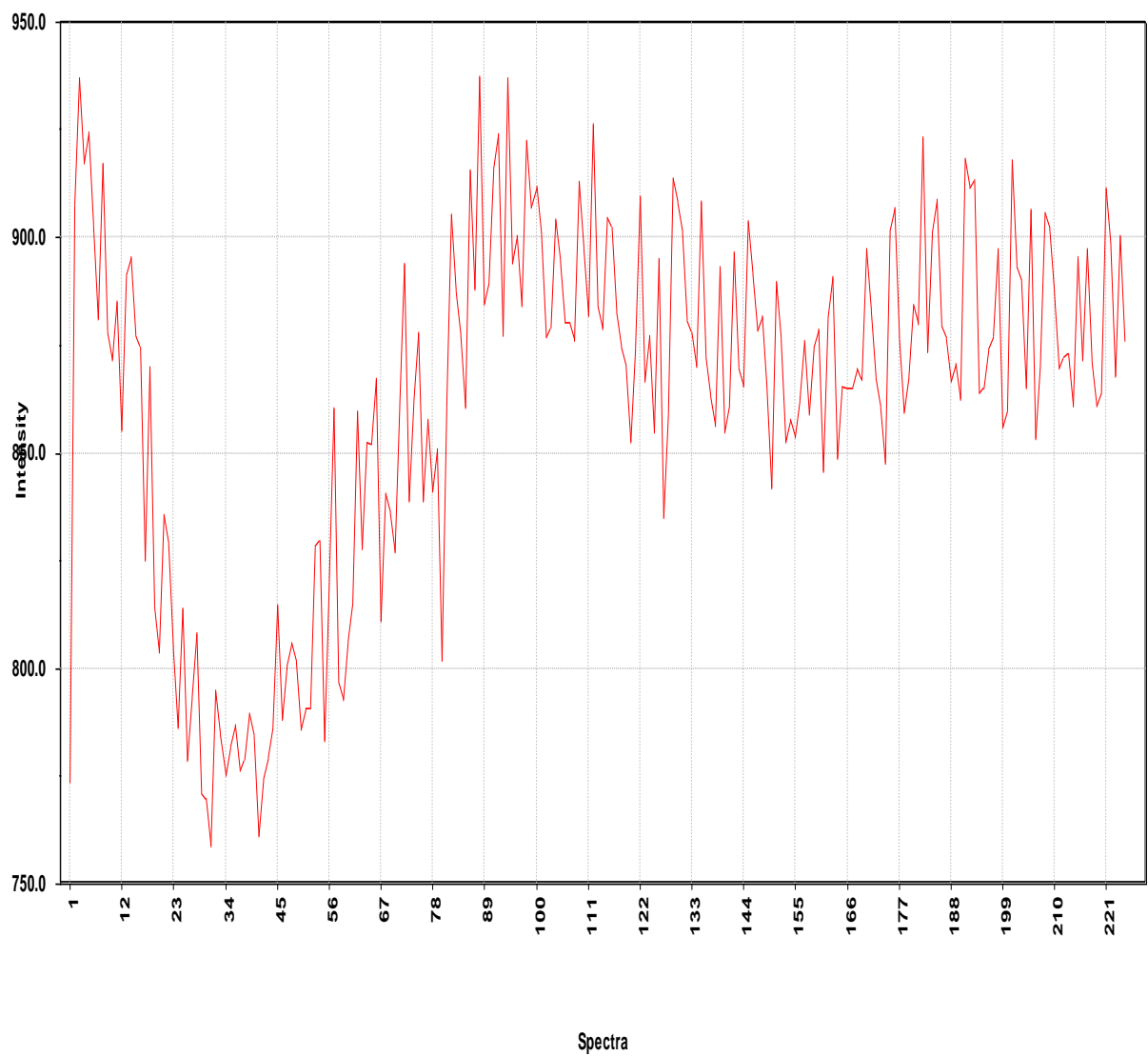


**Figure A9:** Intensity plot for Raman frequency at  $894\text{ cm}^{-1}$  for Reaction 3 under the batch conditions

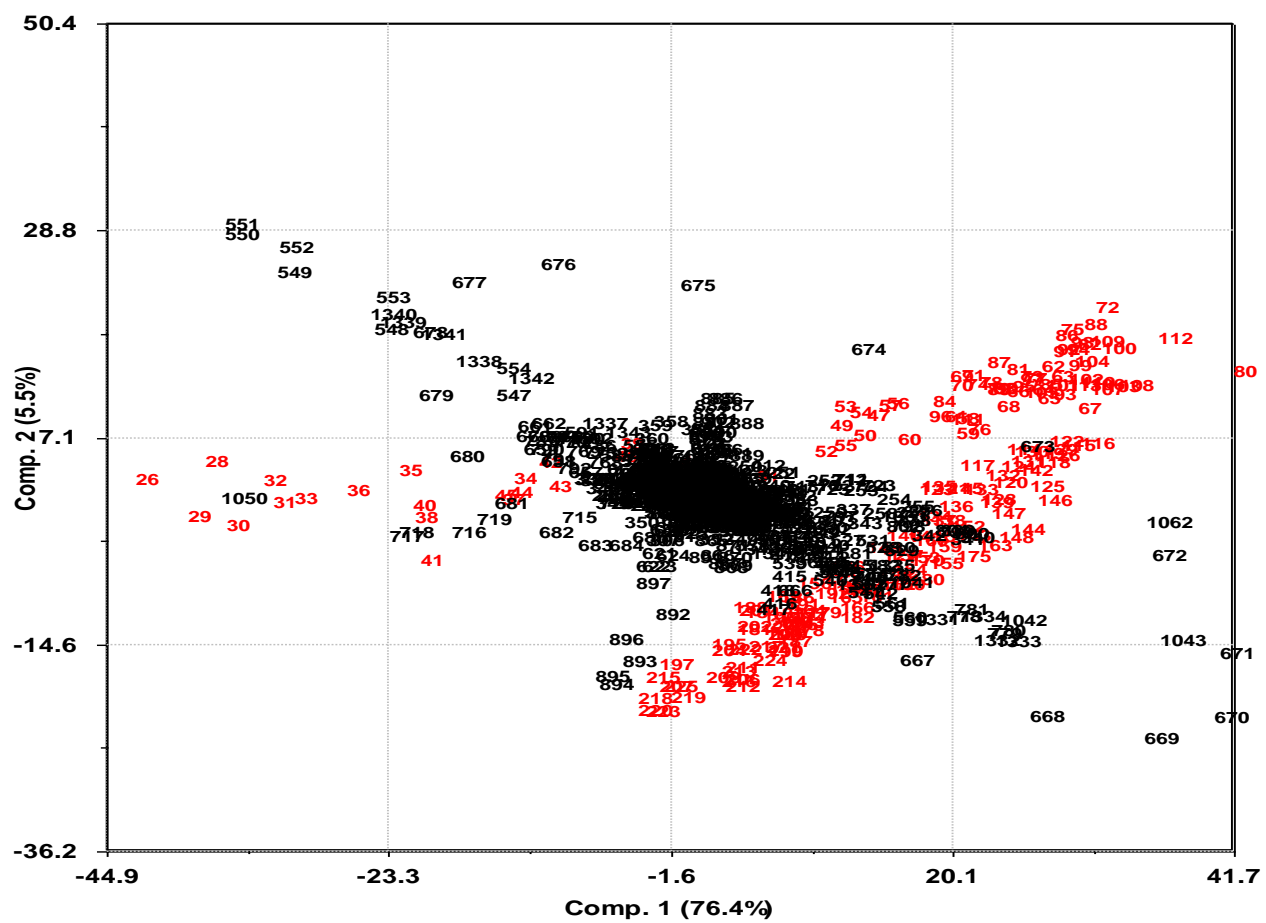


**Figure A10:** Biplot for Reaction 3 under the batch conditions

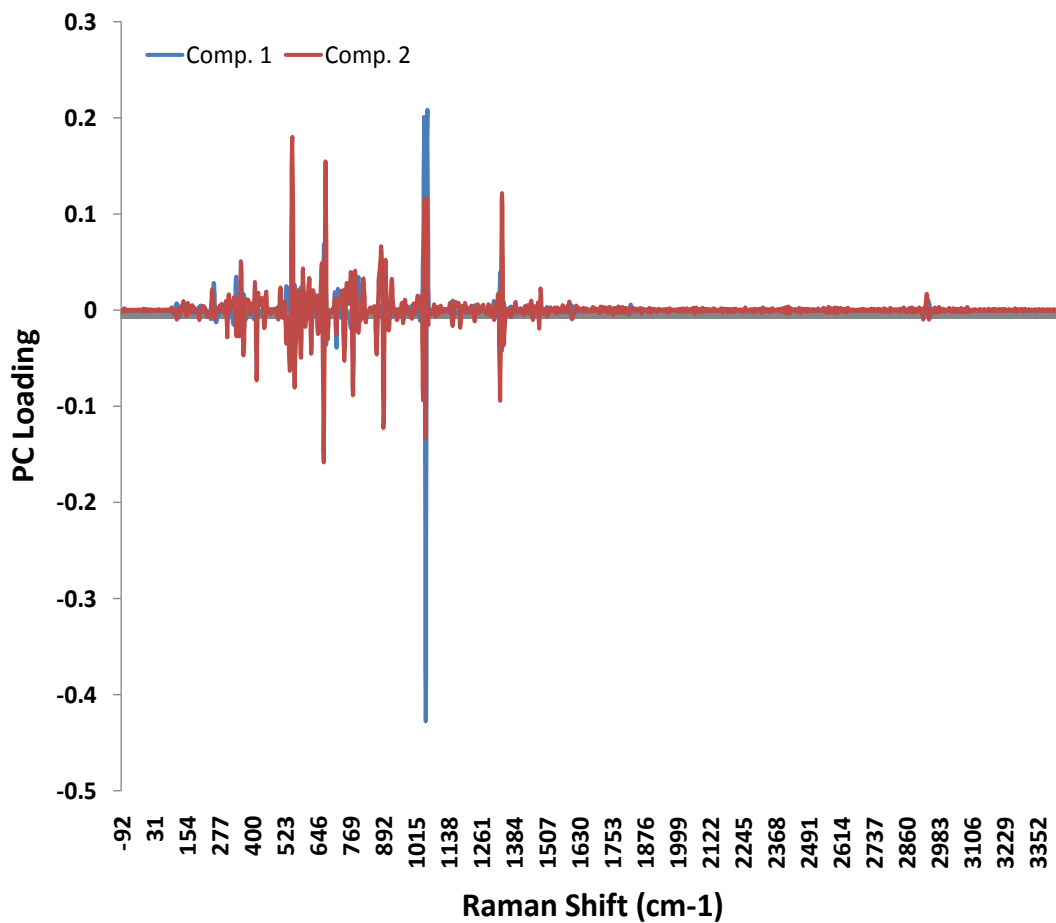


**Figure A11:** Loading plot for Reaction 3 under the batch conditions

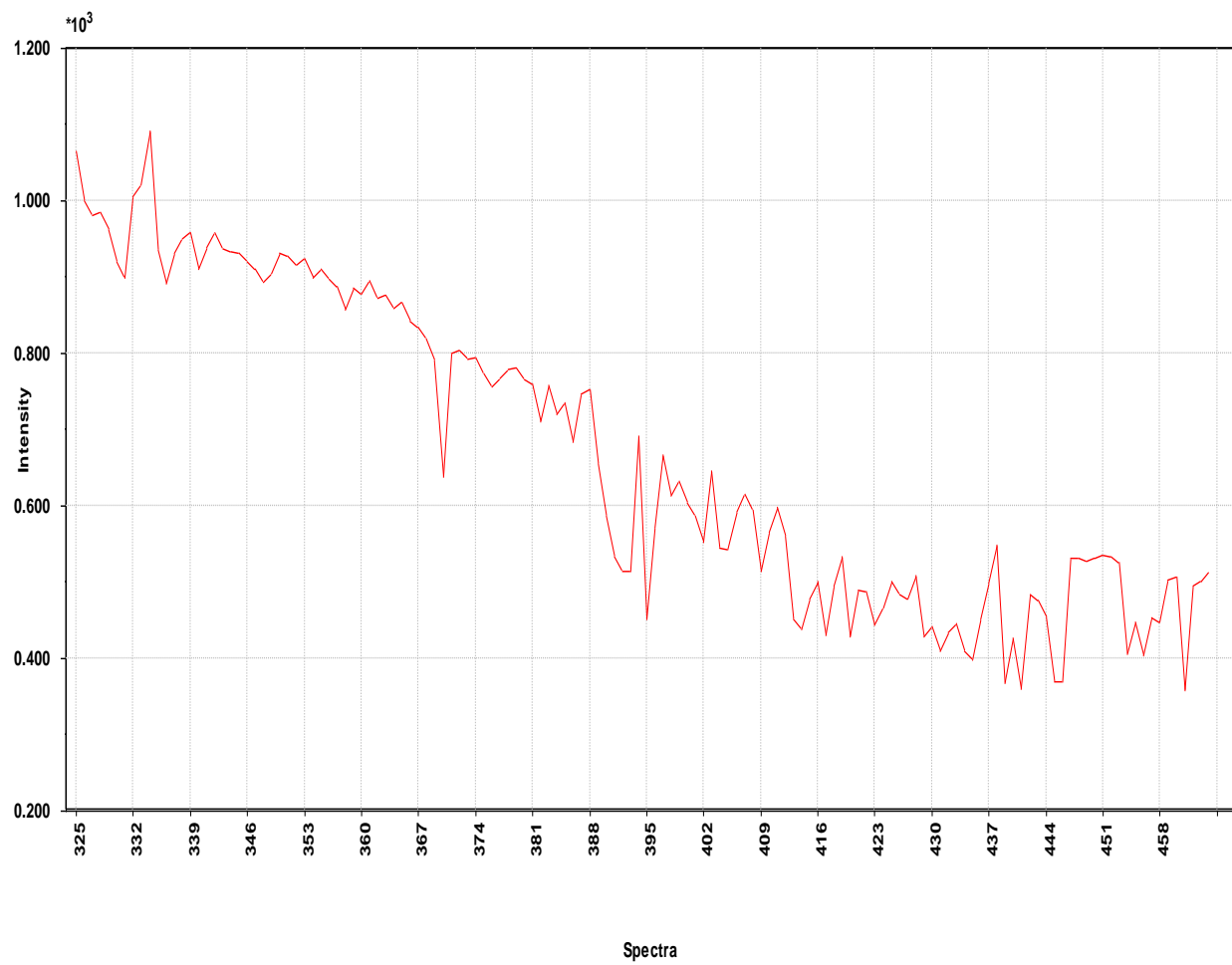


**Figure A12:** Intensity plot for Raman band at  $894\text{ cm}^{-1}$  for the first run in reactor for Reaction 3